MOLECULAR AND CELLULAR BIOLOGY, Sept. 2010, p. 4463–4479 Vol. 30, No. 18
0270-7306/10/$12.00 doi:10.1128/MCB.01207-09

Type I Phosphatidylinositol Phosphate Kinase Beta Regulates Focal Adhesion Disassembly by Promoting β1 Integrin Endocytosis▽

Wei-Ting Chao,[1] Felicity Ashcroft,[2] Alexes C. Daquinag,[1]† Tegy Vadakkan,[1] Zhubo Wei,[1] Pumin Zhang,[1] Mary E. Dickinson,[1] and Jeannette Kunz[1]*

Department of Molecular Physiology and Biophysics[1] and Department of Molecular and Cellular Biology,[2] Baylor College of Medicine, 1 Baylor Plaza, Houston, Texas 77030

Received 7 September 2009/Returned for modification 4 October 2009/Accepted 27 May 2010

Cell migration requires the regulated disassembly of focal adhesions, but the underlying mechanisms remain poorly defined. We have previously shown that focal adhesion disassembly requires the dynamin 2- and clathrin-dependent endocytosis of ligand-activated β1 integrins. Here, we identify type I phosphatidylinositol phosphate kinase beta (PIPKIβ), an enzyme that generates phosphatidylinositol-4,5-bisphosphate ($PI4,5P_2$), as a key regulator of this process. We found that knockdown of PIPKIβ by RNA interference blocks the internalization of active β1 integrins and impairs focal adhesion turnover and cell migration. These defects are caused by the failure to target the endocytic machinery, including clathrin adaptors and dynamin 2, to focal adhesion sites. As a consequence, depletion of PIPKIβ blocks clathrin assembly at adhesion plaques and prevents complex formation between dynamin 2 and focal adhesion kinase (FAK), a critical step in focal adhesion turnover. Together, our findings identify PIPKIβ as a novel regulator of focal adhesion disassembly and suggest that PIPKIβ spatially regulates integrin endocytosis at adhesion sites to control cell migration.

Cell migration is a highly dynamic process that depends on the ability of a cell to adhere to and deadhere from the extracellular matrix in a coordinated manner. Adhesion is mediated through focal adhesion sites, which assemble in response to activation and clustering of integrin receptors and comprise signaling and scaffolding proteins, such as focal adhesion kinase (FAK), talin, vinculin, paxillin, and zyxin (9, 55). These complexes anchor the extracellular matrix to the actin cytoskeleton and also serve as signaling platforms (9, 55). The formation of adhesive complexes is essential for the stabilization of membrane protrusions and to provide the tensile forces for migration (9, 55). However, rapid cell movement requires that focal adhesions not only be continuously formed, but also disassembled (9, 56). The coordinated control of cell adhesion, and release thereof, is therefore a critical regulatory function for migrating cells. However, while much has been learned about the mechanisms underlying focal adhesion assembly, comparatively little is known about how the turnover of adhesion sites is regulated, despite the importance of this process for cell migration.

Recently, the protease calpain, FAK, and phosphatases and kinases that control the activity of FAK, as well as microtubules and the large GTPase dynamin 2, have been identified as regulators of focal adhesion disassembly (9, 10, 21, 22). In particular, a pathway has been defined in which microtubule targeting of focal adhesions leads to their disassembly (21). A critical step in this process is the formation of a protein complex between FAK and dynamin 2, a key regulator of endocytosis (21). Dynamin 2, together with components of the clathrin machinery, then mediates the turnover of focal adhesions by promoting the internalization of β1 integrins (14, 41). Notably, dynamin 2 and clathrin adaptors become enriched at focal adhesion sites prior to their disassembly (14, 21). Therefore, mechanisms that control the recruitment of the endocytic machinery to focal adhesion sites must exist. However, how this process is regulated during focal adhesion turnover remains unknown.

Phosphatidylinositol-4,5-bisphosphate ($PI4,5P_2$) has recently emerged as an important regulator of focal adhesion dynamics (38, 47, 51, 57). In addition to serving as the precursor to other second messengers, $PI4,5P_2$ directly binds and modulates many focal adhesion components, including talin, vinculin, and α-actinin, that regulate adhesion assembly and their linkage to the actin cytoskeleton (38, 47, 51, 57). Adhesion to the extracellular matrix stimulates the synthesis of $PI4,5P_2$, and the general paradigm has been that the resulting local increase in $PI4,5P_2$ levels promotes focal adhesion assembly (23, 38, 40). Intriguingly, emerging evidence suggests that $PI4,5P_2$ also promotes the disassembly of focal adhesions (13, 46). This finding implies that $PI4,5P_2$ levels at adhesion sites must be tightly regulated, both spatially and temporally, to elicit its specific, yet inverse, effects on focal adhesion dynamics.

The generation of $PI4,5P_2$ at specific subcellular sites is modulated in part by the selective targeting and activation of specific type I phosphatidylinositol phosphate kinases (PIPKI), which synthesize $PI4,5P_2$ (38). Three related PIPKI isoforms, designated PIPKIα, PIPKIβ, and PIPKIγ, and multiple splice variants are present in mammalian cells (27, 28, 39, 49). Recent studies have shown that the increase of $PI4,5P_2$ synthesis leading to focal adhesion assembly is mediated through the specific recruitment of PIPKIγ661, a splice variant of PIPKIγ, to focal adhesions (18, 37). However, whether PIPKIγ661 or another

* Corresponding author. Mailing address: Department of Molecular Physiology and Biophysics, Baylor College of Medicine, One Baylor Plaza, BCM335, RM T419, Houston, TX 77030. Phone: (713) 315-1980. Fax: (713) 798-3475. E-mail: jkunz@bcm.tmc.edu.

† Present address: The Brown Foundation Institute of Molecular Medicine for the Prevention of Human Disease, University of Texas Health Science Center at Houston, Houston, TX.

▽ Published ahead of print on 12 July 2010.

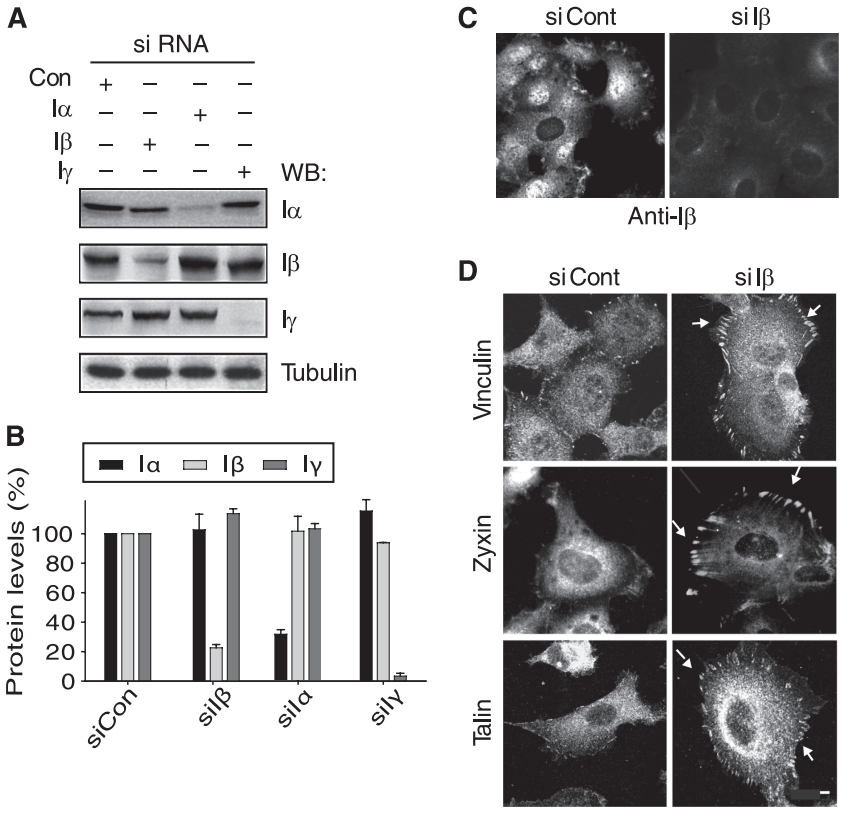

FIG. 1. PIPKIβ knockdown leads to the accumulation of stable focal adhesions. (A) Specificity and efficiency of PIPKI protein knockdown. Cell lysates from HT1080 cells were transfected with the indicated siRNAs and subjected to SDS-PAGE and Western blot (WB) analysis using specific antibodies. Con, control. (B) The Western blot band intensity from panel A was determined by quantitative densitometry to determine the level of each PIPKI protein and of tubulin as a loading control. The data shown are representative of three independent experiments. The error bars indicate SEM. (C) Control (Cont) and PIPKIβ-depleted cells were fixed, and the efficiency of PIPKIβ protein knockdown was determined by immunofluorescence analysis using an isoform-specific antibody to PIPKIβ. (D) The distribution of focal adhesion proteins was examined in control and PIPKIβ-depleted cells by immunostaining them with antibodies against vinculin, zyxin, and talin. Arrows indicate focal adhesions accumulating in PIPK1β-depleted cells. All scale bars, 10 μm.

member of the PIPKI family is responsible for synthesizing the $PI4,5P_2$ pool regulating focal adhesion disassembly is currently unknown, and the molecular mechanisms whereby $PI4,5P_2$ regulates this process are not well defined.

Coincidently, $PI4,5P_2$ is also an important organizer of clathrin assembly at the plasma membrane (17). In this study, we therefore set out to determine whether $PI4,5P_2$ promotes focal adhesion disassembly through its effects on endocytosis and to identify the PIPKI isoform involved in generating this pool of $PI4,5P_2$. We show that knockdown of one specific PIPKI isoform, PIPKIβ, blocks adhesion turnover leading to the inhibition of cell migration. We further show that PIPKIβ is necessary for the uptake of activated β1 integrins and provide evidence that $PI4,5P_2$ produced by PIPKIβ orchestrates the recruitment of components of the endocytic machinery to adhesion sites. Together, these studies define the role of $PI4,5P_2$ in the regulation of focal adhesion disassembly and identify PIPKIβ as the enzyme synthesizing this pool of $PI4,5P_2$.

MATERIALS AND METHODS

Antibodies, reagents, and plasmids. Isoform-specific polyclonal rabbit anti-PIPKIβ antibodies were generated against the carboxy-terminal PIPKIβ tail and were affinity purified before use. Mouse antivinculin and antitalin and rabbit antizyxin antibodies were from Sigma (St. Louis, MO); mouse antiphosphotyrosine (4G10) was from Zymed (San Francisco, CA); mouse anti-FAK, mouse anti-phospho-FAK-Y397, and mouse anti-dynamin 2 antibodies were from BD Transduction Laboratories (Lexington, KY); rabbit polyclonal anti-dynamin 2 antibodies were a gift from Mark A. McNiven (Mayo Clinic, Rochester, MI); mouse anti-human β1 integrin 12G10 and MAB1981 antibodies were from Chemicon; Cy2- and Cy3-conjugated goat anti-mouse and Cy2-conjugated goat anti-rabbit IgGs were obtained from Jackson ImmunoResearch (West Grove, PA); and Alexa Fluor 647- or 594-conjugated phalloidin was from Molecular Probes (Invitrogen, Carlsbad, CA). Plasmids containing epitope-tagged wild-type human PIPKIα, PIPKIβ, PIPKIγ635, PIPKIγ661, or the kinase-dead PIPKIβ-KD mutant were previously described (16, 32), and murine EYFP-PIPKIα was from ATCC (Manassas, VA). We use the human PIPKI nomenclature throughout the article, which is different from the mouse designation, as human and mouse PIPKIα and PIPKIβ isoforms were named in a reciprocal manner, i.e., human PIPKIα corresponds to mouse PIPKIβ and *vice versa*. GFP-dynamin 2(aa) was a gift from Mark A. McNiven (Mayo Clinic, Rochester, MI), whereas the dynamin 2 (K44A) mutant was obtained from S. Schmid (Scripps, San Diego, CA). Cherry-zyxin was cloned in the laboratory of Victor Small (IMBA, Vienna, Austria) and was kindly provided by Irina N. Kaverina (Vanderbilt Medical Center, TN). Plasmids containing mRFP-Rab5 and alpha 5 integrin-green fluorescent protein (GFP) were obtained from Addgene.

Plasmid construction. Plasmids containing GST fusions to the isolated pleckstrin-homology (PH) domains of wild-type dynamin 2 or the $Dyn2^{PH}$ mutant were generated by subcloning PCR fragments encoding the PH domains of wild-type dynamin 2 or the $Dyn2^{PH}$ mutant in frame into the polylinker of pGEX-5X (Promega, Madison, WI). The $Dyn2^{PH}$ mutant containing a single substitution (K535A) was created using the QuikChange site-directed mutagenesis kit (Stratagene, La Jolla, CA) according to the manufacturer's protocol.

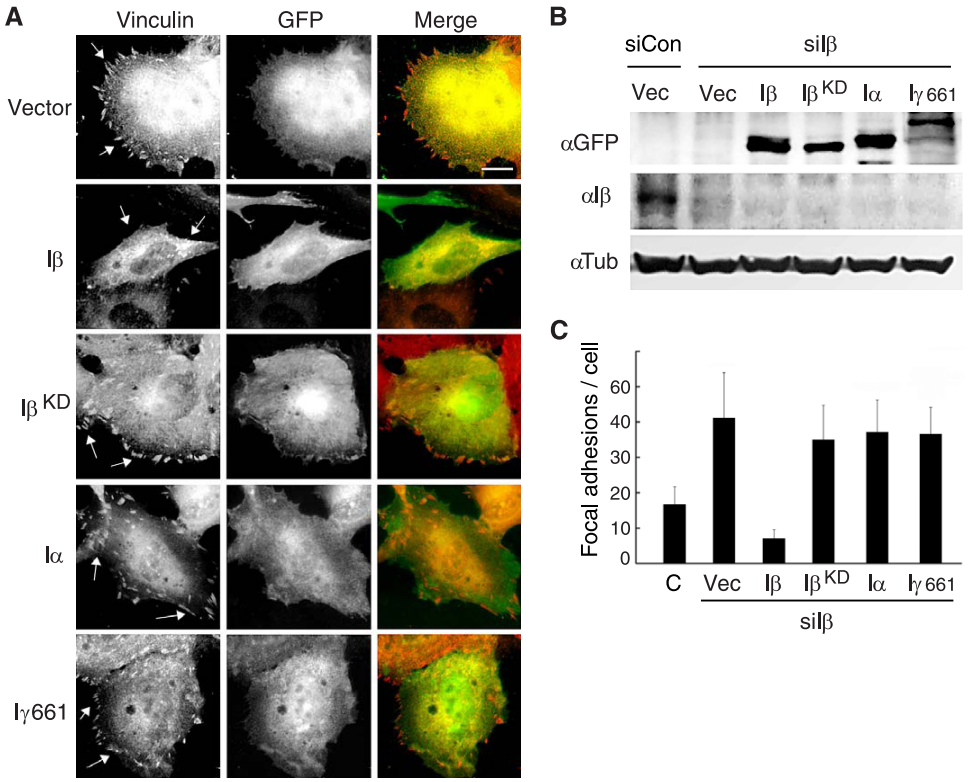

FIG. 2. The role of PIPKIβ in focal adhesion disassembly is isoform specific and requires kinase activity. (A) Comparison of the efficiencies of GFP (Vector) or the GFP-tagged wild-type (Ib) or kinase-dead PIPKIβ (Ib^{KD}) variant and wild-type PIPKIα (Ia) or PIPKIγ661 (Ig661) in rescuing the focal adhesion defect of PIPKIβ-depleted cells. Transfected cells were fixed and immunostained for vinculin (red) to visualize adhesions (arrows). GFP fluorescence (green) was recorded directly. Bar, 10 μm. (B) Western blot analysis of cell lysates from panel A to confirm expression of transfected cDNAs and the efficacy of PIPKIβ knockdown. As a control, tubulin levels remained constant. Vec, vector. (C) Quantitative analysis of vinculin focal adhesion numbers from panel A. The results are the means plus SEM (n = 3).

Human GFP-dynamin 2(aa) was used as a template. A cDNA fragment containing the Dyn2^{PH} open reading frame was then digested with appropriate restriction enzymes and cloned in frame into the polylinker of pEGFP-C1. The nucleotide sequences of all constructs were verified by DNA sequencing.

Cell culture. The human fibrosarcoma HT1080 cell line (ATCC) was grown in Dulbecco's modified Eagle's Medium (DMEM) supplemented with 10% calf serum, penicillin, and streptomycin (GIBCO-BRL, Gaithersburg, MD) with 5% CO_2 at 37°C.

siRNA transfection. Small interfering RNA (siRNA) Smart-pool reagents (a mixture of four oligonucleotides specific for each targeted gene) were purchased from Dharmacon. The siGenome Smart-pool reagents used were as follows: PIPKIα, M004780-02-0010; PIPKIβ, M004058-00-0005; PIPKIγ, M004782-00-0005; dynamin 2, M004007-01-0005; and scrambled control siRNA (siCont), D-001810-10-05. siRNA pools were transfected at a final concentration of 100 nM (single duplexes at 25 nM) into 30 to 50% confluent HT1080 cells grown on 24-well plates in normal growth medium without antibiotics using Lipofectamine 2000 (Invitrogen, CA) as recommended by the manufacturer. siRNA-treated cells were typically analyzed 48 h posttransfection. The efficacy of RNAi knockdown was confirmed by reverse transcription (RT)-PCR with specific primers and by immunoblot analysis of lysates using appropriate antibodies.

Immunofluorescence analysis and confocal time lapse imaging. Cells grown on glass coverslips were fixed with 3.7% formaldehyde, permeabilized in 0.1% Triton X-100, and incubated with primary (1:50 to 1:100 dilution in PBS-0.1% Triton X-100-3% bovine serum albumin [BSA]) and appropriate secondary antibodies (1:200 dilution in PBS-0.1% Triton X-100-3% BSA). Coverslips were mounted with Gel Mount aqueous mounting medium (Sigma, St. Louis, MO). Images were acquired using a Zeiss LSM 510 META confocal microscope with a 63× objective (1.4 numerical-aperture [NA] oil). The live imaging was carried out at 37°C in an environmental chamber using a Nikon A1R microscope with a 60× objective (1.49 NA oil). The pinhole was set to 1 airy unit, and the 488 and 561 lasers were used in line series to excite the GFP and Cherry fusion proteins, respectively. For image processing, background extraction was applied to the entire time series based on a region of interest outside the cell.

Focal adhesion disassembly assay. Focal adhesion disassembly assays were performed as described previously (21) with minor modification. At the indicated times, cells were fixed in paraformaldehyde, permeabilized, and immunostained with mouse monoclonal antibodies against focal adhesion markers (vinculin, FAK-pY397, or zyxin) or a rabbit polyclonal antibody directed at dynamin 2, followed by appropriate secondary antibodies. To visualize microtubules, cells were fixed in −20°C methanol for 10 min, rehydrated in Tris-buffered saline (TBS), and stained with a mouse monoclonal antibody against tubulin and an appropriate secondary antibody. The focal adhesion number represents the mean and standard error of the mean (SEM) from approximately 150 cells in each group. The number of focal adhesions in each cell was evaluated from photographs of vinculin staining. The data shown are representative of three independent experiments.

Cell spreading assay. Cells were detached with 0.02% EDTA in Dulbecco's phosphate-buffered saline (DPBS) without Ca^{2+} or Mg^{2+} (Sigma) and replated onto plastic culture dishes coated with 10 μg/ml fibronectin. After 45 min, cells (n = 1,000) were counted, and the percentage of spread cells was evaluated. Nonspread cells were defined as round phase-bright cells, whereas spread cells were defined as those that lacked a round shape, were not phase bright, and had extended membrane protrusions. Data from at least three independent experiments were collected.

Transwell migration assay. siRNA-treated HT1080 cells (1×10^5) were plated in the upper chamber of a transwell chamber (8.0-μm pore size; BD Transduction Laboratories). For haptotaxis assays, the underside of the filter was coated with fibronectin (10 μg/ml). Cultures were incubated for 2 h at 37°C, and nonmigrating cells were then removed from the top chamber with cotton swabs, and the remaining cells were fixed for 20 min in 3.7% formaldehyde–0.5% Triton X-100 in DPBS, stained with DAPI (4′,6-diamidino-2-phenylindole) to visualize nuclei, and mounted, and cells from eight different areas were counted by

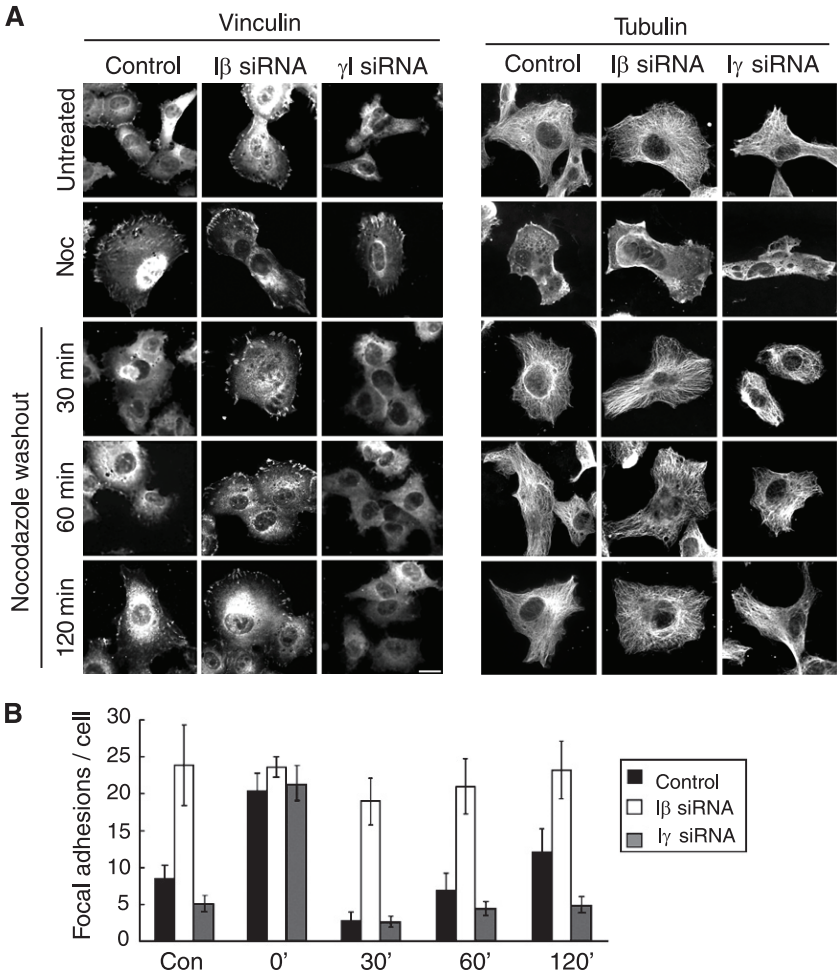

FIG. 3. PIPKIβ is required for microtubule-dependent focal adhesion disassembly. (A) HT1080 cells were transfected with scrambled control siRNAs or siRNAs targeting PIPKIβ or PIPKIγ, serum starved, and left untreated or incubated with nocodazole (Noc) (10 μM; 1 h at 37°C). The cells were then fixed before or at the indicated times after nocodazole washout, and focal adhesions (left) and microtubules (right) were visualized by immunostaining with antibodies against vinculin and tubulin, respectively. Bar, 10 μm. (B) Quantification of focal adhesion number during nocodazole treatment and washout from panel A. The values are means ± SEM ($n = 3$).

fluorescence microscopy. Data from at least three independent experiments performed in duplicate were collected.

Determination of RhoA-GTP levels. Cells were treated with scrambled control or PIPKIβ-specific siRNAs and were harvested 48 h later, washed, and lysed with 25 mM Tris, pH 8.0, 25 mM NaCl, 1% Triton X-100, 10% glycerol, and Complete protease inhibitor cocktail (Roche). RhoA-GTP was isolated by pulldown assays with a glutathione *S*-transferase (GST) fusion protein containing the rhotekin Rac-binding domain as described previously (44). Bound RhoA was analyzed using SDS-PAGE and Western blotting. The blots were developed using an enhanced-chemiluminescence system (SuperSignal West Dura Extended Duration Substrate [Pierce]). The RhoA levels from three independent experiments were quantified by scanning densitometry using the Image Gauge 4.0 program, and multiple exposures of each gel were analyzed. RhoA-GTP levels were normalized against total RhoA in the cell lysate.

Liposome binding assays. Wild-type and mutant GST-PH domains expressed in BL21 cells as a fusion protein with GST were purified on glutathione-Sepharose 4B gel (Amersham Bioscience, Piscataway, NJ) and eluted using a standard procedure. Phosphoinositide vesicles were prepared as a mixture of $PI4,5P_2$ with phosphatidylcholine (PC) by sonication and extrusion, essentially as described previously (1). Purified GST fusions at various concentrations were then incubated with a 500-μM total lipid concentration (PC:$PI4,5P_2$ liposome containing 15 mol% $PI4,5P_2$). After incubation of liposomes with GST fusion proteins, liposomes were centrifuged at 100,000 × *g*, and the pellet and supernatant fractions were isolated and separated by SDS-PAGE. GST fusion proteins were visualized by staining them with Coomassie brilliant blue. The Coomassie-stained bands were quantitated using a Li-Cor (Lincoln, NE) Odyssey imaging system V.1.2.

β1 integrin internalization. β1 integrin endocytosis was measured essentially as described previously (29), with minor modifications. HT1080 cells were grown on coverslips and starved for 2 h at 37°C in DMEM lacking serum but containing 0.5% BSA. For steady-state experiments, the cells were then incubated at 37°C for 2 h with mouse anti-human integrin-β1 antibody (5 μg/ml; 12G10, Chemicon), which recognizes the extracellular domain of activated human β1 integrin. Unbound antibodies were removed by washes, and the cells were fixed with 3.7% (vol/vol) paraformaldehyde in phosphate-buffered saline (PBS), permeabilized, and immunostained using rabbit antizyxin followed by Cy3-conjugated secondary antibodies. For pulse-chase experiments, serum-starved HT1080 cells were pretreated with nocodazole (10 μM; 1 h; 37°C) and then incubated with anti-human integrin-β1 antibody 12G10 for 1 h at 4°C in the presence of nocodazole. Unbound antibodies and nocodazole were then washed away, and the chase was performed in complete medium containing 10% fetal bovine serum (FBS) at 37°C for the indicated times. To quantify β1 integrin internalization, noninternalized surface antibodies were removed prior to fixation by an acid rinse (0.5% acetic acid, 0.5 M NaCl, pH 3.0, for 20 to 30 s). Internalized β1 integrin-antibody conjugates were directly visualized with Cy2-conjugated goat anti-mouse antibodies. All images were acquired under identical parameters using a Zeiss LSM 510 META confocal microscope with a 63× objective (1.4 NA oil; Zeiss). Serial *z* sections were obtained from individual cells every 0.5 μm, and the total

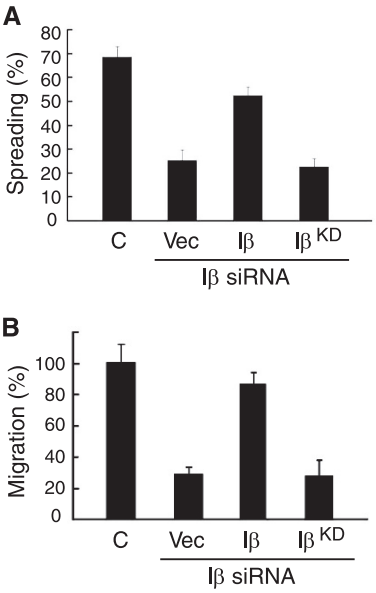

FIG. 4. PIPKIβ is required for cell spreading and migration. (A) PIPKIβ-depleted cells, transfected with empty vector or plasmids containing wild-type or kinase-dead PIPKIβ variants, were plated on fibronectin-coated culture dishes and allowed to spread for 45 min. The percentage of spread cells is indicated and compared to that of control cells transfected with scrambled control (C) siRNAs. At least 1,000 cells were counted per experiment ($P < 0.01$; $n = 3$). (B) Control siRNA-treated or PIPKIβ-depleted cells were transfected with the indicated plasmids, serum starved, and assayed for cell migration across 8-μm Transwell membranes in response to serum (10% FBS). The results are expressed as the percentage of migrated cells relative to the percentage of migrated control siRNA-treated cells, which was arbitrarily set to 100%. The values are means plus SEM ($P < 0.01$; $n = 3$).

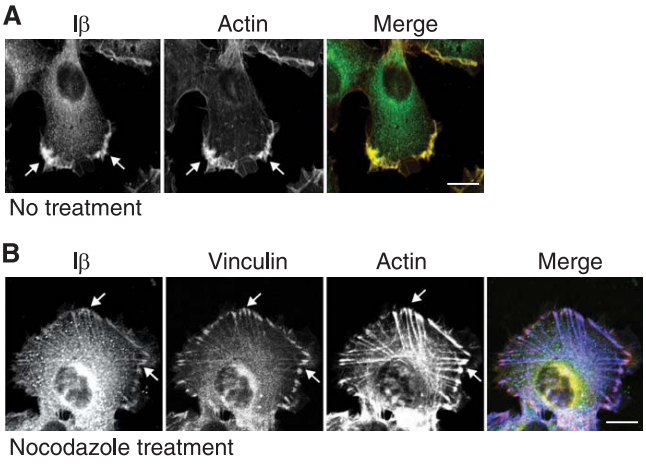

FIG. 5. Endogenous PIPKIβ targets to stable focal adhesions. (A) Migrating HT1080 cells were fixed and stained with an isoform-specific antibody to PIPKIβ and with phalloidin to visualize F-actin. Endogenous PIPKIβ protein localized to the plasma membrane (arrows) and vesicle-like structures. (B) Nocodazole-treated HT1080 cells were fixed and stained with antibodies to PIPKIβ and vinculin. The actin cytoskeleton was visualized with phalloidin. The results revealed colocalization of PIPKIβ with vinculin at focal adhesions (arrows) and along the ends of actin stress fibers. Bars, 10 μm.

fluorescence intensity per cell area for the projected confocal *z* sections was measured as described previously (41) using LSM 5 Pascale software to determine the mean level of internal β1 integrin. Data were collected from 40 cells per condition sampled from three independent experiments.

Surface biotinylation assays. Surface biotinylation and detection of β1 integrins by capture enzyme-linked immunosorbent assay (ELISA) were performed essentially as described previously (45) with minor modifications. Serum-starved HT1080 cells were pretreated with nocodazole (10 μM; 1 h; 37°C). Cell surface proteins were then biotinylated using EZ-link Sulfo-NHS-SS-Biotin (Pierce, IL) in PBS at 4°C for 30 min. Labeled cells were washed twice in cold PBS and then incubated at 37°C in serum-free medium for various periods of time for internalization, after which biotin groups remaining on the cell surface were cleaved off by three 20-min washes at 4°C with reducing buffer (100 mM sodium-2-mercaptoethane sulfonate, 50 mM Tris, pH 8.6, 100 mM NaCl). The cells were then washed three times in cold PBS and lysed in RIPA buffer. Biotinylated β1 integrin was captured on streptavidin ELISA plates (Nunc immobilizer; Nunc, Roskilde, Denmark) from the cell lysates diluted to 10 μg/ml total protein in PBS containing 0.5% Tween 20 (PBST) for 1 h of incubation at room temperature. The plates were then washed three times with PBST and incubated with anti-human integrin-β1 antibody 12G10 for 1 h. After three washes with PBST, the plates were incubated with horseradish peroxidase (HRP)-conjugated anti-mouse secondary antibody for 1 h and washed three times in PBST, and the HRP signal was revealed by incubation with OPD color substrate (Sigma, St. Louis, MO). Color development was stopped by adding an equal amount of 3 M H_2SO_4 and was analyzed at 492 nm using an ELISA reader. For surface integrin detection, nocodazole-treated cells were labeled at 4°C for 30 min with EZ-link Sulfo-NHS-SS-Biotin as described above. Immediately thereafter or after nocodazole washout for 30 min, the cells were transferred to ice to arrest endocytosis. To label cell surface integrins, the cells were then incubated with anti-human integrin-β1 antibody 12G10 at 4°C for 1 h, followed by washes with cold PBS and incubation with HRP-conjugated anti-mouse antibodies for an additional 1 h. Cells were collected and lysed, the cell lysates were incubated in streptavidin ELISA plates for 1 h at room temperature to capture biotinylated proteins, and the integrin signal was detected using OPD substrate as described above.

Rescue experiments. HT1080 cells were transfected with siRNA pools as indicated in the text and incubated in 10% FBS medium. Thirty-six hours post-transfection, the cells were retransfected with cDNAs encoding enhanced yellow fluorescent protein (EYFP)-tagged murine orthologs of the indicated human PIPKI isoforms or mutant variants thereof or with wild-type or mutant dynamin 2. Transfection with empty vector was used as a control. The transfection efficiency in these experiments was typically 90% as judged by green fluorescent protein (GFP) fluorescence. The transfected cells were incubated in serum-free medium for 12 h and were then assayed for cell spreading, cell migration, or focal adhesion disassembly or were incubated in normal growth medium and assayed for β1 integrin internalization.

Coimmunoprecipitation and Western blot studies. For coimmunoprecipitation studies, HT1080 cells were lysed in lysis buffer (1% NP-40, 50 mM Tris [pH 7.4], 150 mM NaCl, 2 mM $MgCl_2$, 1 mM EGTA, and protease and phosphatase inhibitors), and endogenous active FAK was immunoprecipitated with anti-pY397-FAK antibody (4 μg mouse monoclonal/1 mg cell lysate; BD Transduction) essentially as described previously (21). Immunoprecipitation with an equal amount of IgG from normal rabbit serum served as a specificity control. In some cases, cell lysates were prepared 12 h posttransfection from cells that transiently expressed Flag-tagged wild-type or mutant variants of dynamin 2, and endogenous pY397-FAK was immunoprecipitated from these lysates as described above. The immunoprecipitates and total cell lysates were then separated by SDS-PAGE and analyzed by Western blotting for the presence of pY397-FAK (mouse monoclonal; 1:3,000; BD Transduction) and copurifying endogenous dynamin 2 (rabbit polyclonal; 1:1,000; M. McNiven) or transfected Flag-tagged dynamin 2 variants (M5 monoclonal anti-Flag antibody, 1:1,000; Kodak), followed by appropriate HRP-conjugated secondary antibodies (1:15,000; Jackson ImmunoResearch). The blots were developed with SuperSignal (Pierce, Rockford, IL) and exposed on Kodak Scientific Imaging Film.

Quantification of dynamin 2 localization. To quantify focal adhesion association of wild-type and mutant dynamin 2 variants, focal adhesion areas (defined as areas enriched in the focal adhesion marker zyxin) at the cell periphery were randomly selected, and a circular area of fixed diameter was overlaid over each area (120 pixels in diameter). The average pixel intensity of the circular area was then measured for the dynamin 2 channel. The value obtained was considered to represent focal-adhesion-targeted dynamin 2. The same measurement was performed on a corresponding nearby peripheral region devoid of the focal adhesion marker zyxin to obtain the background value of dynamin 2 not associated

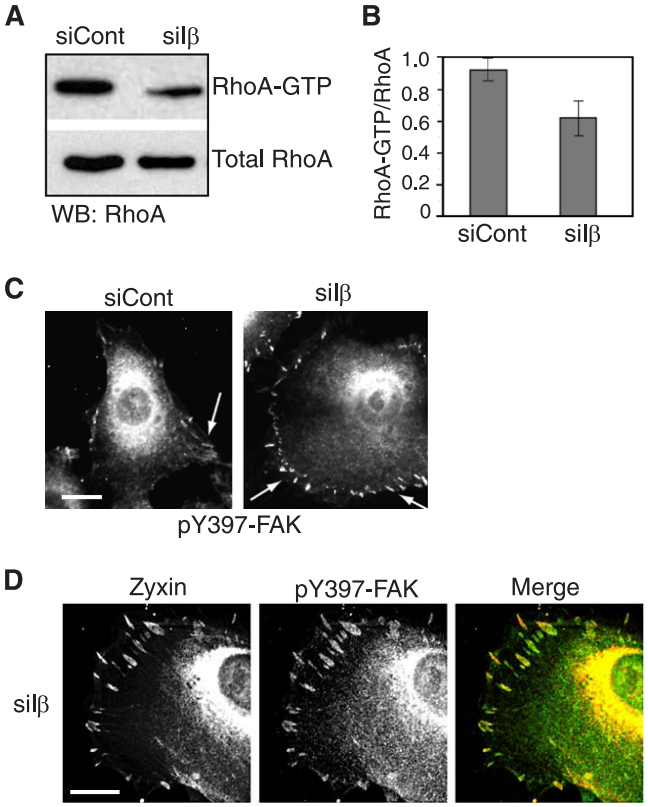

FIG. 6. Effects of PIPKIβ knockdown on RhoA and FAK activation. (A) RhoA-GTP levels were measured in control or PIPKIβ-depleted cells by pulldown assay with rhotekin-RBD-coated beads, followed by immunoblotting with anti-RhoA antibodies. The expression levels of total RhoA are shown below. (B) Quantitation of the amount of GTP-RhoA relative to total RhoA levels under each condition based on Western blot band intensity quantification. The error bars indicate SEM. (C) The localization of activated FAK was visualized by immunostaining using a phosphorylation-specific antibody specific for pY397-FAK. PIPKIβ knockdown cells accumulated enlarged focal adhesions enriched in pY397-FAK (arrows) relative to control scrambled siRNA-transfected cells. (D) PIPKIβ-depleted cells were immunostained with antibodies against pY397-FAK and the focal adhesion marker zyxin, followed by appropriate fluorescently labeled secondary antibodies. Bars, 10 μm.

with focal adhesions. This value was deducted from the first measurement. Several areas (3 to 5) were measured for 50 randomly chosen cells.

Statistics. All statistics of quantification in this study, including spreading assay, Transwell migration assay, and focal adhesion numbers, were performed by Student's *t* test.

RESULTS

PIPKIβ is required for focal adhesion disassembly. To identify the PIPKI isoform necessary for the disassembly of focal adhesions, we used RNA interference (RNAi) to silence the expression of each of the three PIPKI family members individually in the human fibrosarcoma HT1080 cell line. This led to the specific and efficient (~80% at the protein level) downregulation of each targeted kinase without affecting the levels of nontargeted PIPKIs (Fig. 1A and B). PIPKI-deficient cells were then stained for a panel of focal adhesion markers, including vinculin, talin, and zyxin. We found that only cells depleted of PIPKIβ showed an increase in the number of prominent focal adhesions relative to control cells treated with a scrambled siRNA pool (Fig. 1C and D and data not shown), which typically indicates a change in the kinetics of focal adhesion disassembly (26, 54, 55). The focal adhesion phenotype of PIPKIβ knockdown cells could be rescued by the reintroduction of the siRNA-resistant mouse ortholog of PIPKIβ, but not by the related PIPKIα or PIPKIγ661 isoform (Fig. 2A to C), suggesting that PIPKIβ plays an isoform-specific role in the regulation of focal adhesions. Moreover, the role of PIPKIβ in this process was dependent on its ability to generate $PI4,5P_2$, because expression of its kinase-dead mutant ($PIPKI\beta^{KD}$) failed to correct the focal adhesion defect associated with PIPKIβ knockdown (Fig. 2A to C). Collectively, these data suggest that PIPKIβ controls the synthesis of a pool of $PI4,5P_2$ that is critical for the turnover of focal adhesions.

To confirm the role of PIPKIβ in focal adhesion turnover, we took advantage of a method to monitor the synchronized disassembly of adhesion sites (4, 21, 30). This method is based on the finding that microtubule depolymerization upon nocodazole treatment reversibly blocks focal adhesion assembly. Microtubule regrowth after nocodazole washout then induces the rapid disassembly of adhesions in the entire cell population. By using this approach, we found that control siRNA-treated HT1080 cells formed enlarged peripheral adhesions after 1 h of nocodazole treatment, as shown by quantification of vinculin (Fig. 3A and B). These adhesions disassembled in a synchronous manner within 20 to 30 min after nocodazole washout and microtubule regrowth and reappeared within 1 h after nocodazole washout (Fig. 3A and B). Consistent with the idea that depletion of PIPKIβ alone blocks focal adhesion disassembly, PIPKIβ knockdown cells exhibited a significant increase in the number and size of focal adhesions already in the absence of nocodazole, and nocodazole treatment of these cells did not further increase focal adhesion numbers (Fig. 3A and B). More importantly, nocodazole washout failed to induce the turnover of focal adhesions in PIPKIβ-depleted cells, even though microtubule regrowth appeared normal in these cells (Fig. 3A and B). These data therefore confirm that PIPKIβ is necessary for focal adhesion disassembly.

Significantly, the effects caused by PIPKIβ depletion were markedly different from those caused by silencing of PIPKIγ, the only PIPKI member previously implicated in the regulation of focal adhesion dynamics (18, 37). PIPKIγ knockdown cells displayed a significant decrease in focal adhesion numbers (Fig. 3A and B), suggesting that PIPKIγ is necessary for the assembly or stability of adhesion complexes. Consistent with this, focal adhesions accumulated in PIPKIγ-depleted cells following nocodazole treatment, but these adhesions rapidly disassembled after nocodazole washout and failed to reassemble after microtubule regrowth to the cell periphery (Fig. 3A and B). We therefore conclude that PIPKIγ knockdown leads to a defect in the formation of stable focal adhesions but does not affect their disassembly. Collectively, these results provide strong evidence that PIPKIβ and PIPKIγ both modulate focal adhesion dynamics but control different stages of adhesion assembly and disassembly.

PIPKIβ is necessary for cell spreading and migration. The rapid turnover of focal adhesion complexes is essential for efficient cell spreading and migration. We found that the majority of PIPKIβ-depleted cells (~70%) displayed a significant

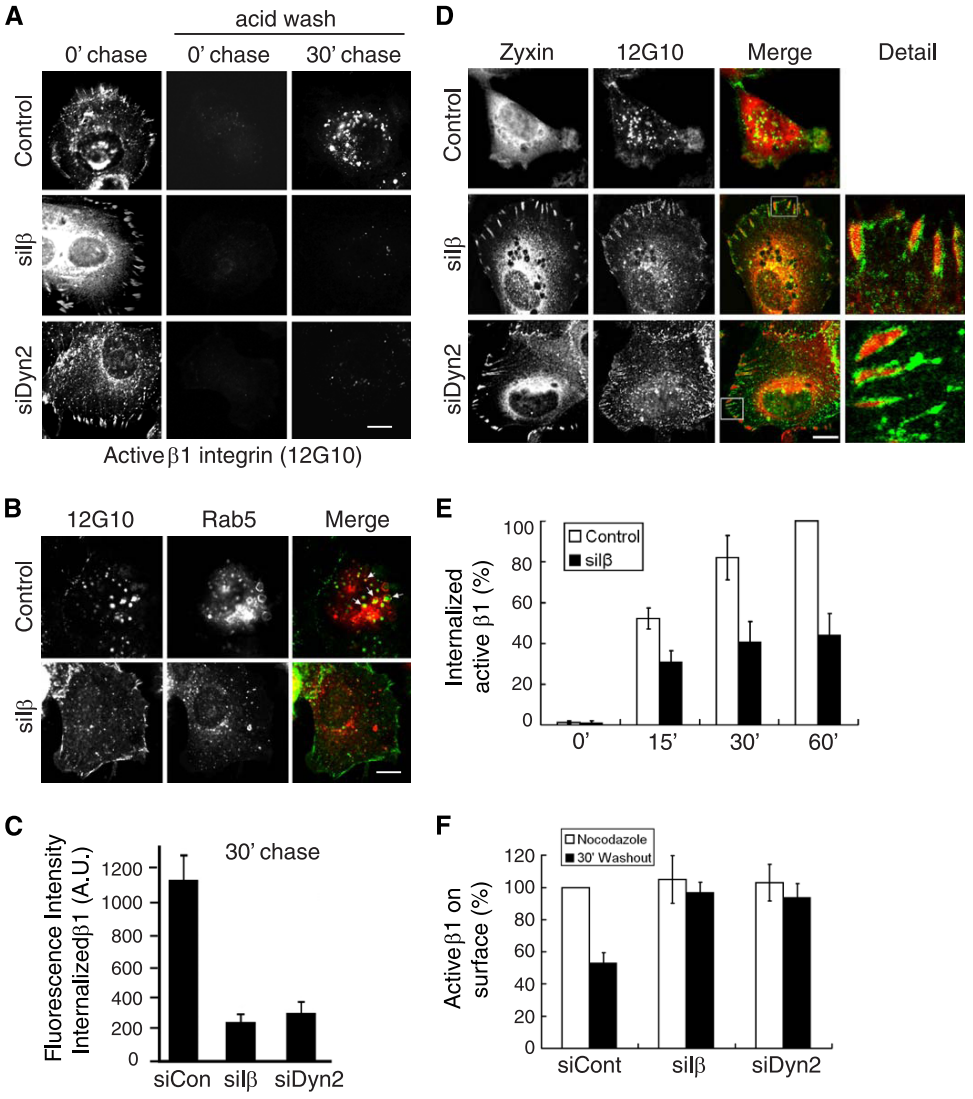

FIG. 7. Knockdown of PIPKIβ blocks the endocytosis of activated β1 integrins. (A) HT1080 cells, transfected with the indicated siRNAs, were treated for 1 h at 37°C with nocodazole. The cells were then incubated for 1 h at 4°C in the continuous presence of nocodazole with 12G10 antibody to label ligand-activated β1 integrins on the cell surface. After nocodazole washout, the cells were either left at 4°C or shifted to 37°C for 30 min to allow internalization of integrin-antibody complexes. 12G10 anti-β1 integrin antibodies were removed from the cell surface by acid wash, the cells were fixed and permeabilized, and internalized β1 integrin-antibody complexes were visualized using appropriate secondary antibodies. (B) HT1080 cells were treated with scrambled control (top) or PIPKIβ-specific (bottom) siRNAs and transfected with DsRed-Rab5. The cells were then treated with nocodazole and incubated with 12G10 antibody as described in the legend to panel A. After nocodazole washout for 20 min, the cells were fixed and the localization of β1 integrin-antibody complexes was detected using appropriate secondary antibodies. The arrows point to intracellular activated (12G10-positive) β1 integrin colocalizing with Rab5. (C) Quantitative analysis of internalized β1 integrin. The fluorescence intensity of internalized β1 integrin from panel A was measured and expressed as arbitrary units (A.U.). The error bars indicate SEM ($n = 3$). (D) siRNA-treated HT1080 cells were incubated in the continuous presence of 12G10 anti-β1 integrin antibody for 2 h at 37°C to allow constitutive internalization of β1 integrin-ligand complexes. The cells were then washed, fixed, permeabilized, and immunostained to visualize zyxin (red in merge) and β1 integrin-antibody complexes (green in merge). The regions outlined by white boxes are shown at higher magnification (Detail) to highlight the clustering of ligand-bound integrins around zyxin-containing adhesions. (E) Internalization of biotinylated active β1 integrin. Nocodazole-treated control or PIPKIβ-depleted cells were surface biotinylated at 4°C. After nocodazole washout, the cells were incubated at 37°C for the indicated times to allow internalization of surface proteins. Biotin was then removed from the cell surface proteins, and internalized biotinylated, ligand-activated β1 integrins were analyzed by capture ELISA with 12G10 antibody. The data show the percentage of internalized active β1 integrin relative to control siRNA-treated cells (mean ± SEM; $n = 3$). (F) Cell surface levels of active β1 integrin. Nocodazole-treated control or dynamin 2- or PIPKIβ-depleted cells were subjected to surface biotinylation at 4°C. Ligand-activated biotinylated β1 integrins residing on the cell surface were then labeled either immediately or after nocodazole washout for 30 min at 37°C with 12G10 antibody, followed by incubation with HRP-conjugated secondary antibody (all at 4°C). Biotinylated proteins were then captured on streptavidin-coated ELISA plates, and antibody-HRP conjugates were detected. The data shown are expressed as percentages of control (mean ± SEM; $n = 3$). Scale bars, 10 μm.

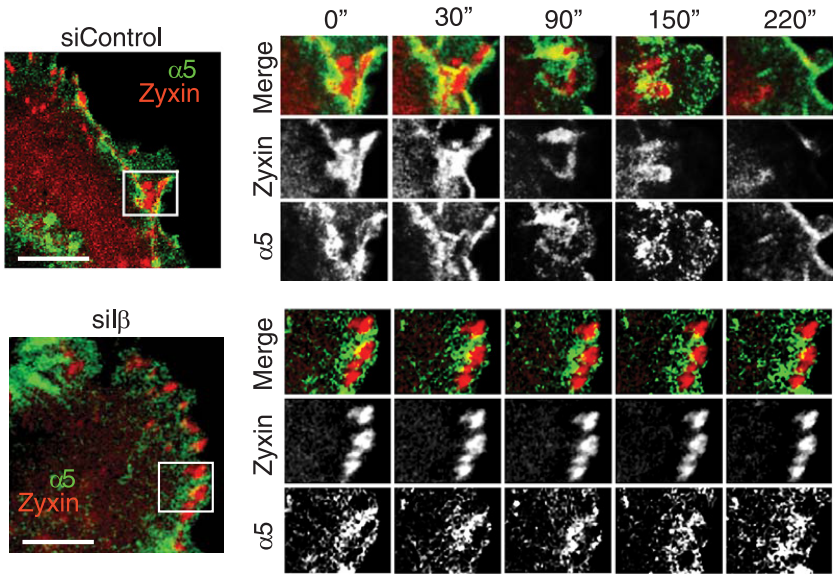

FIG. 8. Dynamics of integrin α5-GFP during focal adhesion disassembly. On the left are merged confocal images of a nocodazole-treated control siRNA-transfected and a PIPKIβ-depleted HT1080 cell transiently expressing integrin α5-GFP (green) and Cherry-tagged zyxin (red). The boxed regions are shown magnified on the right at various time points after nocodazole washout. The times are in seconds starting 6 min after nocodazole washout.

delay in cell spreading on a fibronectin matrix (Fig. 4A) and a marked defect in cell migration toward 10% FBS (Fig. 4B). Both of these defects were rescued by reexpression of wild-type PIPKIβ, but not its kinase-negative variant, in PIPKIβ knockdown cells (Fig. 4A and B), suggesting that the cell spreading and migration defects observed in PIPKIβ knockdown cells are due in part to the dysregulation of PI4,5P_2-dependent focal adhesion disassembly.

PIPKIβ localizes to stable focal adhesions. To assess whether PIPKIβ might affect focal adhesions directly, we examined the subcellular localization of PIPKIβ using isoform-specific antibodies. These antibodies specifically detect PIPKIβ, because siRNA-mediated knockdown of PIPKIβ protein in HT1080 cells strongly reduced the PIPKIβ signal (Fig. 1A to C). Consistent with a previous report (19), endogenous PIPKIβ was detected at the plasma membrane, in intracellular vesicle-like structures, and diffusely throughout the cytoplasm (Fig. 5A). However, when focal adhesion disassembly was arrested by nocodazole treatment, PIPKIβ became enriched along actin stress fibers and at focal adhesions, where it colocalized with vinculin (Fig. 5B). These data show that PIPKIβ targets to stable focal adhesions before focal adhesion disassembly.

PIPKIβ controls the endocytosis of activated integrins. To elucidate the mechanism by which PIPKIβ regulates focal adhesion disassembly, we next tested whether PIPKIβ knockdown affects the activities of key regulators of focal adhesion stability or turnover. First, we examined whether PIPKIβ depletion enhanced RhoA activation, as RhoA is known to stimulate actin stress fiber and focal adhesion formation. However, GTP-RhoA levels were modestly decreased in PIPKIβ-depleted cells relative to control siRNA-treated cells (Fig. 6A and B). This finding is in agreement with a previous report (33) and excludes the possibility that PIPKIβ depletion stabilizes focal adhesions by causing the hyperactivation of RhoA. In addition, phosphorylation of FAK on Tyr397, which is critical for FAK activation and focal adhesion disassembly (21, 24, 55), was not impaired in PIPKIβ-depleted cells relative to control cells, and FAK-pY397 signal was properly enriched in focal adhesions, where it colocalized with zyxin (Fig. 6C and D).

Having excluded negative regulation of FAK as the primary explanation for the observed defect in focal adhesion disassembly, we focused on cellular processes downstream of FAK. We previously showed that the turnover of focal adhesions requires endocytosis of ligand-activated β1 integrins (14). To investigate whether PIPKIβ is necessary for this process, we performed pulse-chase experiments. To this end, PIPKIβ-depleted and control cells were treated with nocodazole to arrest focal adhesion disassembly and were then incubated at 4°C with an antibody (12G10) that specifically recognizes the activated form of the β1 integrin subunit (pulse). After washes to remove nocodazole and unbound antibodies, incubation was continued to allow focal adhesion disassembly (chase). The cells were then acid stripped prior to cell fixation, which efficiently removed antibodies from cell surface integrins (Fig. 7A, 0′ chase). Internalized antibody-integrin complexes were then visualized by indirect immunofluorescence and quantified by determining the mean fluorescence intensity per cell. As expected (14), control cells efficiently internalized activated β1 integrins within 30 min after nocodazole washout (Fig. 7A and C), a period during which focal adhesion disassembly typically is completed. Importantly, double-labeling experiments showed that after nocodazole washout, β1 integrin-antibody complexes were observed in characteristic vesicular structures that also contained mRFP-tagged Rab5 (Fig. 7B), a marker of the early endosome compartment (15), thus providing evidence that cell surface integrins were indeed endocytosed. In contrast, the majority of active β1 integrin in PIPKIβ-depleted cells failed to be internalized after nocodazole

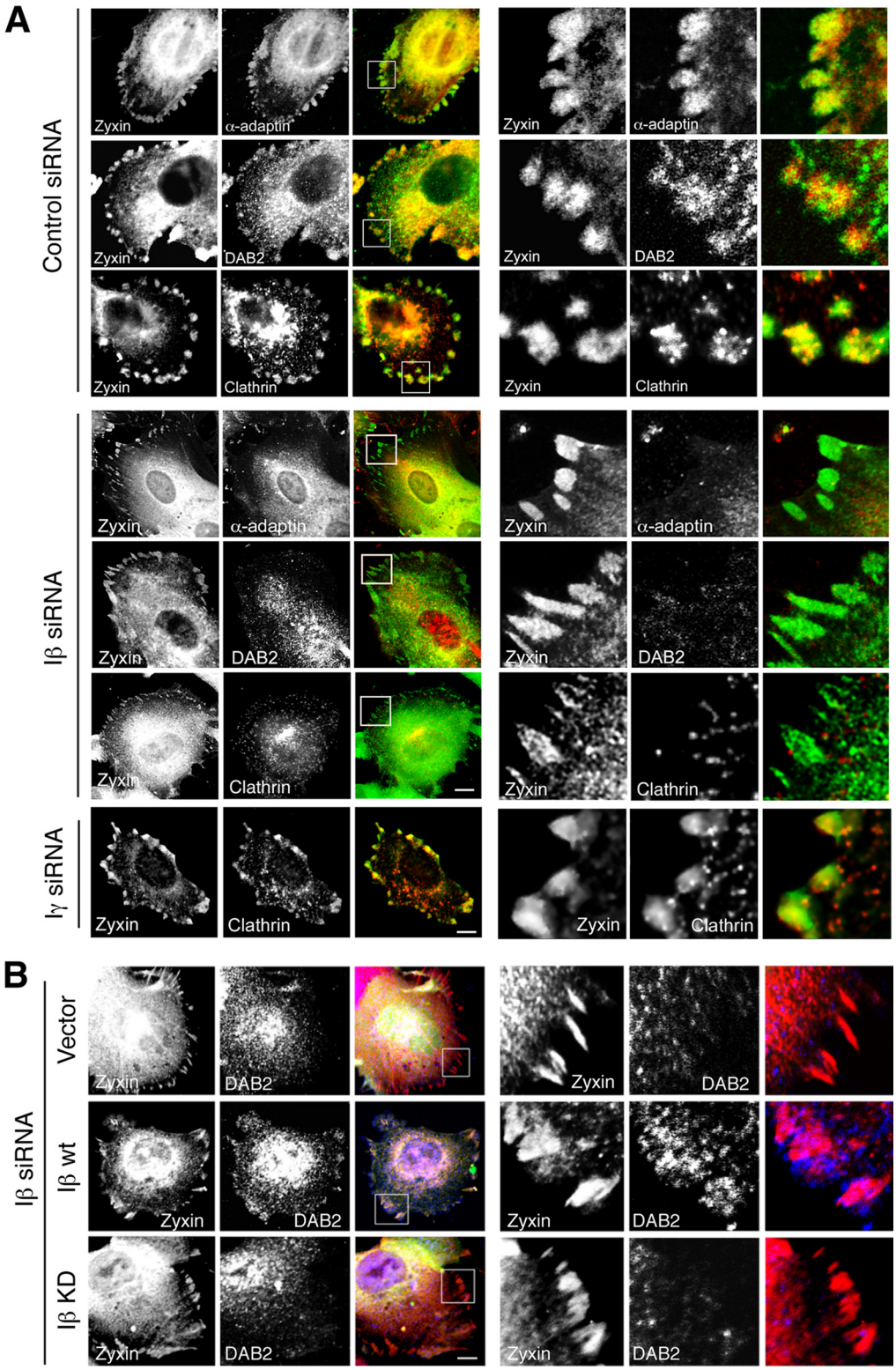

FIG. 9. PIPKIβ is necessary for the recruitment of the clathrin machinery to adhesion sites. (A) HT1080 cells transfected with control siRNAs or with siRNAs targeting PIPKIβ or PIPKIγ were treated with nocodazole to block focal adhesion disassembly. The cells were then fixed, permeabilized, and immunostained to visualize endogenous zyxin (green), DAB2 (red), α-adaptin (red), or clathrin heavy chain (clathrin, red). On the right are shown higher-magnification views of the regions outlined by white boxes on the left. (B) Overexpression of PIPKIβ restores the targeting of clathrin adaptors to focal adhesions. PIPKIβ-depleted cells were transfected with plasmids encoding GFP (Vector), GFP-tagged wild-type (Iβ WT), or kinase-dead PIPKIβ (Iβ KD) variants. The cells were treated with nocodazole to block focal adhesion disassembly and were then fixed and immunostained to visualize endogenous zyxin (red) and DAB2 (blue). GFP fluorescence was recorded directly (green). On the right are shown higher-magnification views of the regions outlined by white boxes. Scale bars, 10 μm.

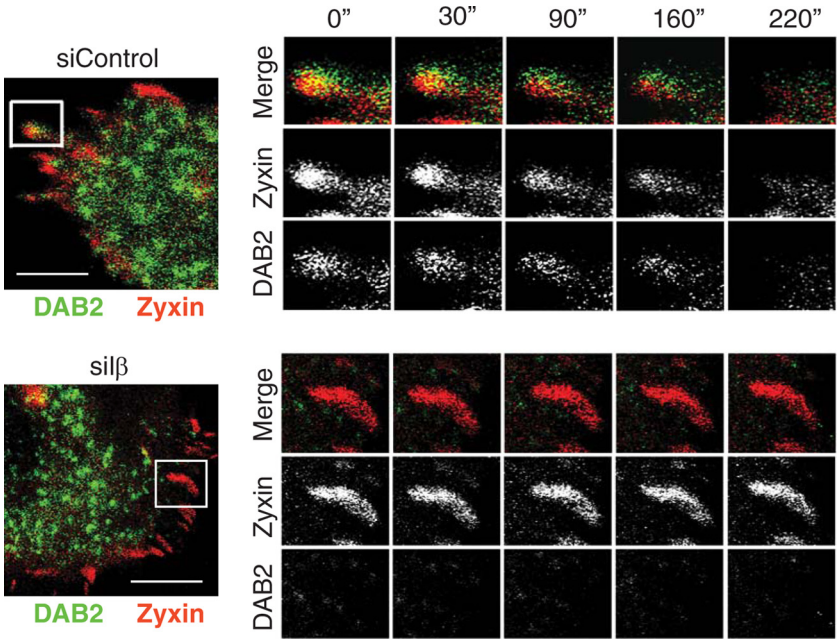

FIG. 10. DAB2 dynamics during microtubule-induced focal adhesion disassembly. HT1080 cells, treated with control siRNAs or PIPKIβ-specific siRNAs, were cotransfected with Cherry-zyxin and GFP-DAB2. The cells were then treated with nocodazole for 1 h, followed by nocodazole washout to induce focal adhesion disassembly. The merged images show confocal images of nocodazole-treated control and PIPKIβ-depleted cells. The outlined regions are shown at higher magnification on the right at different time points during nocodazole washout. The times are in seconds starting 5 min after nocodazole washout to stimulate focal adhesion disassembly.

washout (Fig. 7A and C) and instead remained at the cell periphery (Fig. 7B). Indeed, when integrin uptake was analyzed in the absence of acid stripping, we found that silencing of PIPKIβ led to the retention of β1 integrin-antibody complexes around stabilized zyxin-positive focal adhesions (Fig. 7D). These results suggest that the effect of PIPKIβ on focal adhesion disassembly is mediated through its regulation of β1 integrin internalization. Notably, these effects recapitulated those conferred by the depletion of dynamin 2 (Fig. 7A, C, and D), which is known to be required for β1 integrin endocytosis during focal adhesion disassembly (14).

Because antibody binding may artificially cluster integrins on the cell surface and induce their endocytosis, we also used surface biotinylation to monitor the effect of PIPKIβ knockdown on the internalization of active surface β1 integrins. To do so, nocodazole-treated HT1080 cells were surface labeled with cleavable biotin at 4°C and were then shifted to 37°C for various times to allow endocytosis to occur. The biotin label remaining on the cell surface was then cleaved, and internalized, biotinylated β1 integrins in their active conformation, which were protected from cleavage, were isolated and quantified by capture ELISA analysis using streptavidin and 12G10 antibody. As expected, no β1 integrin was recovered in the biotinylated fraction when biotin was immediately cleaved after surface biotinylation of nocodazole-treated cells (Fig. 7E). However, we observed a significant increase in the recovered biotinylated pool of active β1 integrins in control cells after nocodazole washout, as detected by the 12G10 antibody. This increase was accompanied by a corresponding decrease in the surface levels of activated β1 integrin, suggesting that this pool of integrin is progressively endocytosed (Fig. 7F). In contrast, silencing of PIPKIβ significantly reduced the quantity of internalized active β1 integrins after nocodazole washout (Fig. 7E). This observation was supported by results showing that PIPKIβ loss did not alter the total cell surface pool of active β1 integrins relative to control cells before nocodazole washout but prevented their disappearance from the cell surface after nocodazole washout (Fig. 7F). In sum, these results suggest that PIPKIβ is necessary for the endocytosis of a pool of ligand-activated β1 integrins and that such PIPKIβ-dependent endocytosis is an important regulator of focal adhesion disassembly.

To examine further whether integrins colocalize with zyxin during nocodazole treatment and are removed together with zyxin during focal adhesion disassembly, we monitored the localization of α5β1 integrin, a prominent RGD integrin expressed in HT1080 cells (50). Time-lapse confocal microscopy of cells expressing α5-GFP (34) showed that α5-GFP fluorescence was clustered around peripheral focal adhesions marked by Cherry-zyxin in control cells and PIPKIβ-depleted cells before nocodazole washout (Fig. 8). After nocodazole washout, α5-GFP fluorescence intensity significantly decreased in preexisting adhesion sites within a period of 5 to 10 min in control cells, concomitant with the decrease in Cherry-zyxin signal (Fig. 8), suggesting that α5β1 integrins are removed from these sites during adhesion disassembly. α5-GFP then reemerged at the plasma membrane, indicating that integrins are rapidly exported or recycled (Fig. 8). Under the same conditions, PIPKIβ knockdown cells exhibited little change in focal adhesion intensity and size following nocodazole washout, and the redistribution of α5-GFP integrin from focal adhesions was similarly blocked (Fig. 8). These findings provide

additional evidence that integrins are removed from focal adhesions during focal adhesion disassembly and show that PIPKIβ is necessary for this process.

PIPKIβ regulates the recruitment of clathrin components and dynamin 2 to focal adhesions. Next, we wanted to determine how PIPKIβ modulates β1 integrin endocytosis. We previously showed that focal adhesion disassembly is mediated by a clathrin-dependent mechanism and that clathrin, as well as the clathrin adaptors DAB2 and AP-2, accumulate around focal adhesion sites before adhesion disassembly (14). Significantly, DAB2, as well as the α-adaptin and μ2 subunits of the AP-2 complex, directly binds PI4,5P$_2$, and this is thought to induce their initial membrane recruitment (25, 58). We therefore examined the localization of components of the clathrin machinery in cells that had been treated with nocodazole. As expected (14), clathrin heavy chain, DAB2, and α-adaptin were enriched in the vicinity of zyxin-positive adhesion plaques in control cells (Fig. 9A). In contrast, no enrichment was observed in cells in which PIPKIβ expression had been suppressed (Fig. 9A). PIPKIβ depletion also caused the redistribution of DAB2 and α-adaptin away from focal adhesions (Fig. 9A). Significantly, these effects were observed only upon downregulation of PIPKIβ, whereas silencing of the related PIPKIα (data not shown) or PIPKIγ had no effect on DAB2 and α-adaptin recruitment to adhesion sites (Fig. 9A). We thus conclude that PIPKIβ is specifically required for the targeting of components of the clathrin machinery to focal adhesions. The finding that the clustering of DAB2 (Fig. 9B) and α-adaptin (data not shown) around focal adhesions could be restored to PIPKIβ-depleted cells by expression of wild-type PIPKIβ, but not its kinase-dead mutant variant, further indicates that the targeting of clathrin adapters to focal adhesions is dependent on the synthesis of PI4,5P$_2$.

These observations were supported by analyzing the localization of GFP-tagged DAB2 during focal adhesion disassembly using time-lapse microscopy (Fig. 10). This approach revealed an increase in GFP fluorescence near a subset (~40%) of large focal adhesions in the front and lateral regions of nocodazole-treated control cells (Fig. 10). After nocodazole washout, GFP-DAB2 fluorescence was lost, concomitant with focal adhesion turnover, as evidenced by the delocalization of Cherry-zyxin from adhesion plaques (Fig. 10). In contrast, we did not observe DAB2 fluorescence in focal adhesion areas in PIPKIβ-deficient cells either during nocodazole treatment or after nocodazole washout (Fig. 10). Collectively, these findings support the idea that PIPKIβ facilitates focal adhesion turnover, at least in part, by mediating the recruitment of components of the clathrin machinery to adhesion plaques.

Dynamin 2 is a key effector of PIPKIβ in focal adhesion disassembly. The localization of dynamin 2 to focal adhesions represents a rate-limiting step in focal adhesion disassembly (21). This is thought to be mediated through complex formation with FAK (21). However, dynamin 2 also contains a PH domain, which binds to PI4,5P$_2$ and regulates its membrane insertion (1, 53). Because lipid-protein interactions often act in concert with protein-protein interactions to dock proteins to membranes, we examined whether dynamin's recruitment to focal adhesions is also dependent on PIPKIβ activity. Consistent with such an idea, we found that dynamin 2 failed to accumulate in focal adhesion areas in PIPKIβ knockdown cells prior to adhesion disassembly but was clearly enriched in areas containing zyxin-positive adhesions in control siRNA-treated cells (Fig. 11A). Given that focal adhesion targeting is likely to be important for dynamin's association with FAK, we next determined the effect of PIPKIβ knockdown on the formation of a dynamin 2-FAK complex. To this end, endogenous FAK was immunoprecipitated from lysates derived from control and PIPKIβ-depleted cells and probed for the presence of dynamin 2 by Western blot analysis. We found that dynamin 2 coimmunoprecipitated with FAK in control siRNA-treated cells (Fig. 11B). However, PIPKIβ knockdown cells led to dramatically reduced complex formation, as evidenced by the loss of coimmunoprecipitation (Fig. 11B). We conclude that PIPKIβ is necessary for the efficient recruitment of dynamin 2 to adhesion sites and thereby likely promotes complex formation between dynamin 2 and FAK.

To examine further whether the targeting of dynamin 2 to

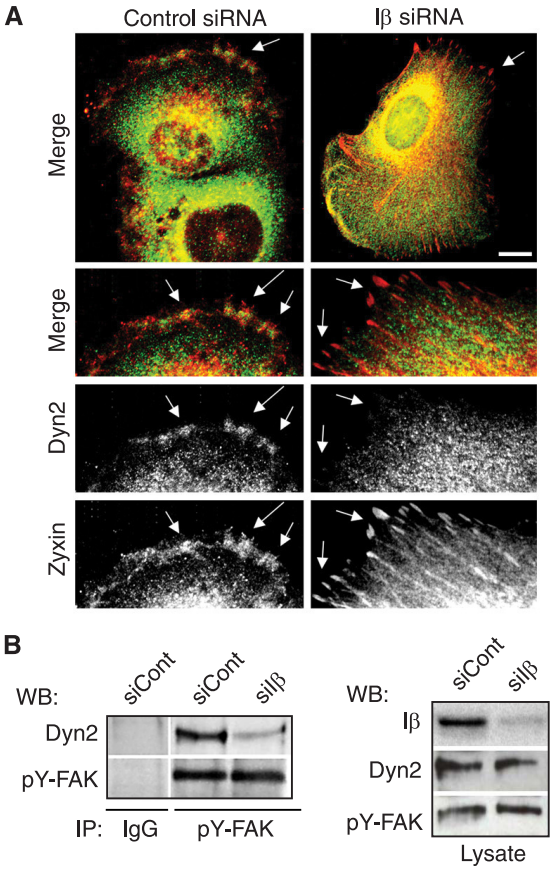

FIG. 11. PIPKIβ is necessary for dynamin 2 localization to focal adhesions and interaction with FAK. (A) Nocodazole-treated control and PIPKIβ-depleted HT1080 cells were immunostained using antibodies against dynamin 2 (green) and zyxin (red). A magnification of the indicated cell area (arrows in top row) is shown below the top images to highlight the lack of dynamin 2 targeting to zyxin-positive focal adhesions (arrows) in PIPKIβ-depleted cells. (B) pY397-FAK was immunoprecipitated (IP) from lysates derived from control or PIPKIβ-depleted cells. The immune complexes, as well as total lysates, were then sequentially analyzed by Western blotting for the presence of endogenous dynamin 2 and pY397-FAK. Control IgG from normal rabbit serum (IgG) served as a control. The efficacy of PIPKIβ knockdown was analyzed by Western blotting of lysates.

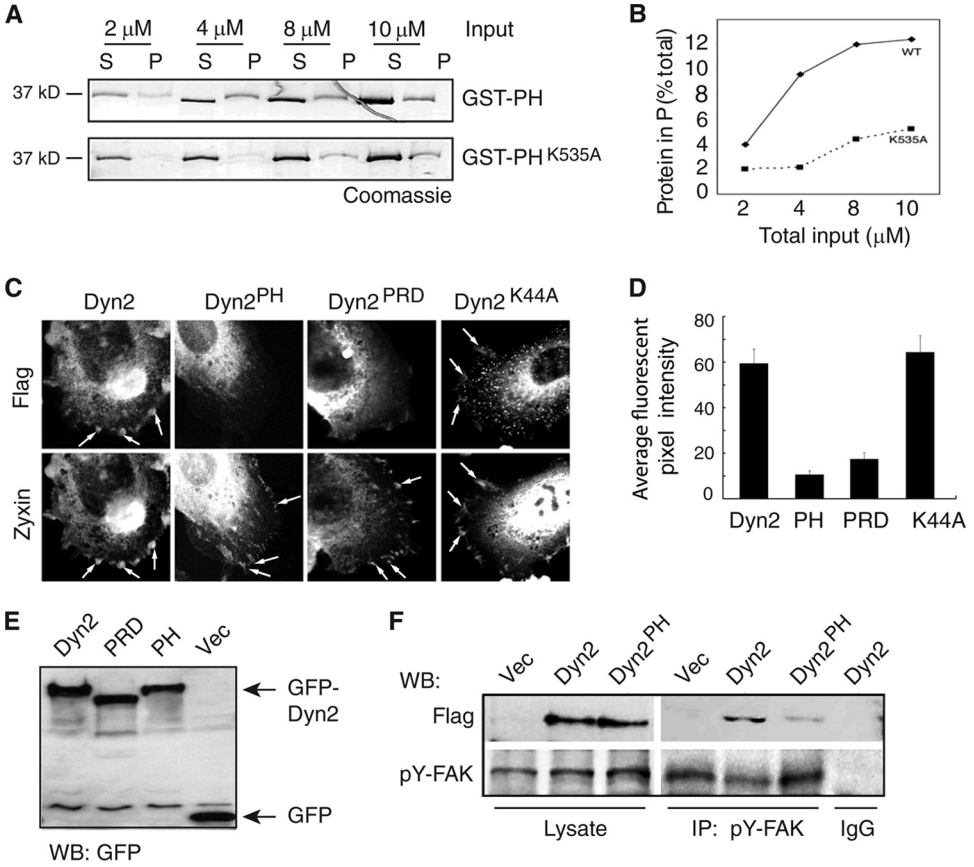

FIG. 12. PI4,5P_2 binding by the PH domain is necessary for dynamin 2 localization to focal adhesions and interaction with FAK. (A) Lys535 is critical for PI4,5P_2 binding by the dynamin 2 PH domain. Purified GST fusion proteins containing wild-type and mutant PH domains of dynamin 2 were incubated at the indicated concentrations with 500 μM liposomes containing 15% (molar) PI4,5P_2 and collected by ultracentrifugation, and pellet (P) and supernatant (S) fractions were analyzed by SDS-PAGE. Proteins were visualized by staining them with colloidal Coomassie. (B) Quantification of the relative protein content in the P fraction. The error bars represent SEM ($n = 3$). (C) HT1080 cells were transfected with Flag-tagged wild-type or mutant dynamin 2 variants and then immunostained with antizyxin and anti-Flag antibodies. The Dyn2^{PH} and Dyn2^{PRD} mutants failed to localize to zyxin-positive adhesions (indicated by arrows). Scale bars, 10 μm. (D) The extent of colocalization of Flag-tagged wild-type and mutant dynamin 2 variants with zyxin was quantitated by measuring the average pixel intensity of Flag fluorescence contained within a focal adhesion area positive for zyxin. The data were compiled from 50 regions analyzed for each construct. The error bars indicate SEM. (E) Western blot analysis of total cell lysates from panel C showing expression of transfected cDNAs. As a control, tubulin levels remained constant. (F) HT1080 cells were transfected with plasmids encoding Flag-tagged wild-type dynamin 2 or the Dyn2^{PH} mutant. pY397-FAK was immunoprecipitated from lysates. The immune complexes, as well as total lysates, were sequentially analyzed by Western blotting for the presence of endogenous dynamin 2, exogenous Flag-tagged dynamin proteins, and pY397-FAK. Control IgG from normal rabbit serum (IgG) served as a control.

focal adhesions is mediated by binding to PI4,5P_2, we generated a mutated form of dynamin 2 that contained a substitution in Lys535 in the PH domain, a key residue necessary for PI4,5P_2 interaction (53) and dynamin function in endocytosis (2, 53). This mutation markedly decreased PI4,5P_2 binding by the isolated mutant PH domain relative to the wild-type PH domain (Fig. 12A and B). To study the functional impact of this mutation, we analyzed the localization of the full-length dynamin 2 mutant variant (designated Dyn2^{PH}) in nocodazole-treated cells and compared it to that of wild-type dynamin 2 or to dynamin 2 variants that lacked GTPase activity (Dyn2^{K44A}) or contained a deletion of the C-terminal PRD domain (Dyn2^{PRD}), which mediates association with FAK (21). We found that both the Dyn2^{PH} mutant and the Dyn2^{PRD} mutant failed to localize to stable focal adhesions prior to focal adhesion disassembly (Fig. 12C and D), whereas wild-type dynamin 2 or the Dyn2^{K44A} mutant was readily detected within adhesion sites. Thus, complex formation with FAK contributes to dynamin's localization to focal adhesion sites; however, this interaction is insufficient to sustain dynamin's association with these sites without the independent contribution of the dynamin-PI4,5P_2 interaction. Moreover, the loss of PI4,5P_2 binding by the dynamin 2 PH domain impaired dynamin's association with FAK. Accordingly, the expression of the Flag-Dyn2^{PH} mutant in HT1080 cells did not lead to stable association of dynamin 2 with FAK, as judged by the absence of coimmunoprecipitation of the Dyn2^{PH} mutant with FAK (Fig. 12F). In contrast, Flag-tagged wild-type dynamin 2 efficiently coprecipitated with FAK (Fig. 12F). As a consequence, the Dyn2^{PH} mutant failed to suppress the focal adhesion defect associated with the depletion of dynamin 2 (Fig. 13A to C) and also failed to reverse the cell migration defect of dynamin

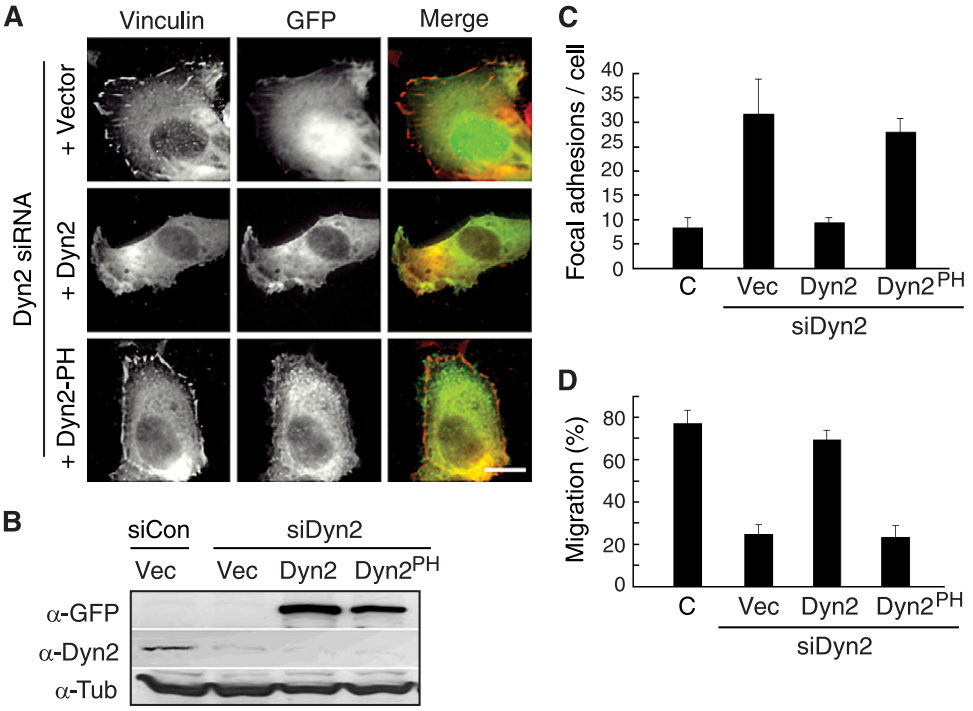

FIG. 13. Dynamin 2 is an effector of PI4,5P$_2$ in focal adhesion disassembly. (A) PI4,5P$_2$ binding by the dynamin 2 PH domain is necessary for focal adhesion disassembly. Dynamin 2-depleted cells were transfected with plasmids encoding GFP (Vector), GFP-tagged wild-type dynamin 2 (Dyn2), or the Dyn2^{PH} mutant. The cells were fixed and immunostained for vinculin. GFP fluorescence was recorded directly. Representative examples of cells are shown (n = 3). (B) Western blot analysis of total cell lysates showing expression of transfected cDNAs and efficacy of dynamin knockdown. As a control, tubulin levels remained constant. (C) Quantitation of focal adhesion numbers from panel A. The values are means plus SEM from three independent experiments in which more than 250 cells were counted. (D) Wild-type dynamin 2, but not the Dyn2^{PH} mutant, suppresses the cell migration defect of dynamin 2 knockdown cells. Cells treated with control or dynamin 2-specific siRNAs were transfected with the indicated plasmids and assayed for cell migration toward 10% serum. The values are means plus SEM (n = 3). The migration of control siRNA-transfected cells was arbitrarily set as 100%.

2-depleted cells (Fig. 13D). Collectively, these results show that dynamin 2 is a critical effector of PI4,5P$_2$ in focal adhesion disassembly.

The notion that PIPKIβ and dynamin 2 act together in a pathway to promote focal adhesion disassembly was supported further by the finding that overexpressed wild-type dynamin 2, but not the Dyn2^{PH} mutant or vector alone, acted as a suppressor of PIPKIβ and corrected the β1 integrin endocytosis defect (Fig. 14A to D), as well as the focal adhesion phenotype associated with PIPKIβ knockdown (Fig. 15A to C). Importantly, ectopic expression of dynamin 2 in PIPKIβ-depleted cells also restored normal cell spreading and migration to these cells (Fig. 15D and E). Collectively, these data support the idea that dynamin 2 is a critical effector of PIPKIβ in focal adhesion disassembly and suggest that the cell migration and spreading defects of PIPKIβ knockdown cells result, at least in part, from the reduced endocytosis of activated β1 integrins.

DISCUSSION

In this report, we identify PIPKIβ as a novel regulator of focal adhesion disassembly and provide evidence that PIPKIβ regulates this process by promoting the endocytosis of ligand-activated integrins. This conclusion is supported by the analysis of integrin endocytosis in PIPKIβ-depleted cells by antibody internalization assay and by surface biotinylation. Confocal microscopy experiments further showed that focal adhesion markers and α5β1 integrins redistribute together from the cell surface into vesicular structures in control cells, but not in PIPKIβ-deficient cells, after nocodazole washout. Collectively, these results consistently suggest that PIPKIβ loss leads to a delay or block in the internalization of ligand-activated β1 integrins and the inhibition of focal adhesion disassembly.

Our results further argue that a primary role of PIPKIβ in focal adhesion disassembly is to regulate the PI4,5P$_2$-dependent recruitment of the clathrin machinery and of dynamin 2 to adhesion sites. Such a model is supported by data showing that PIPKIβ localizes to stabilized focal adhesions and that PIPKIβ activity is essential for the recruitment of the clathrin adaptors DAB2 and AP-2 and of dynamin 2 to membrane domains surrounding adhesion complexes. This conclusion is in line with reports showing that the association of both clathrin adaptors (25, 58) and dynamin (43) with membranes is dependent on PI4,5P$_2$. Based on these findings, we propose that PIPKIβ creates membrane domains enriched in PI4,5P$_2$ at focal adhesions that act as platforms to recruit and functionally organize components of the endocytic machinery. In doing so, PI4,5P$_2$ may initiate and orchestrate the formation and fission of endocytic vesicles at or near focal adhesion sites to promote the internalization of activated β1 integrin receptors. Consistent

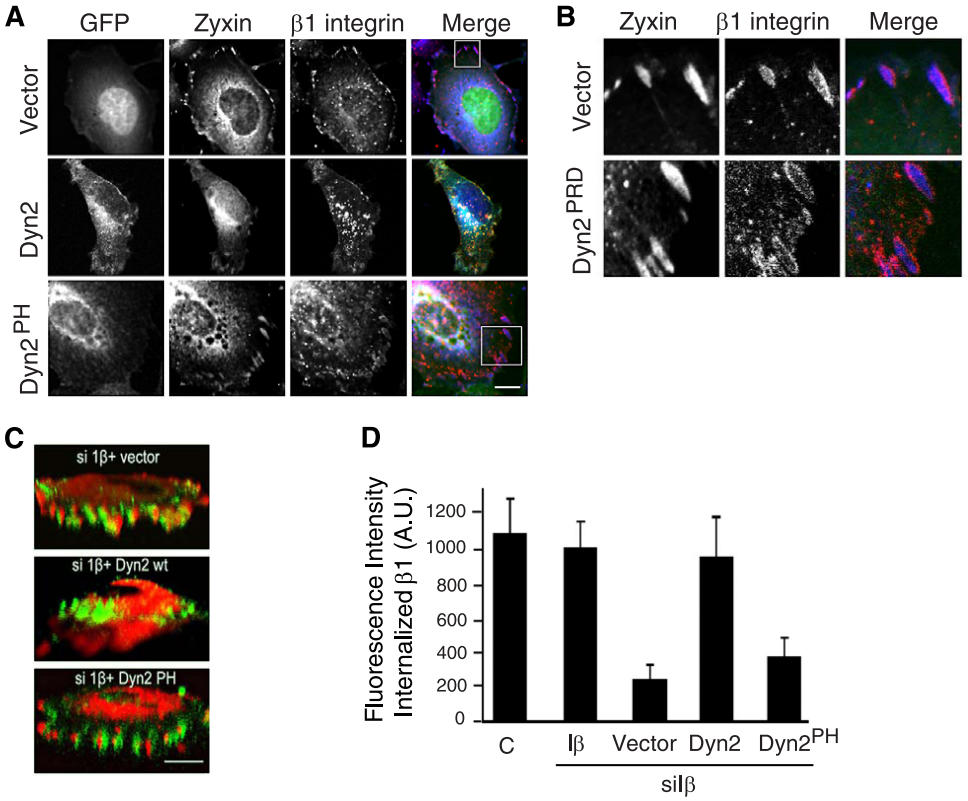

FIG. 14. Dynamin 2 overexpression suppresses the endocytosis defect associated with PIPKIβ knockdown. (A) Overexpression of dynamin 2, but not the $Dyn2^{PH}$ mutant, restores β1 integrin internalization to PIPKIβ-depleted cells. PIPKIβ-depleted cells were transfected with plasmids encoding GFP (Vector), GFP-tagged wild-type dynamin 2 (Dyn2), or the $Dyn2^{PH}$ mutant and were then incubated in the presence of 12G10 anti-β1 integrin antibody for 2 h at 37°C to allow internalization of β1 integrin-ligand complexes. The cells were then immunostained to visualize zyxin (blue) and activated β1 integrin-antibody complexes (red). GFP fluorescence was recorded directly (green). Representative confocal *z* sections at the substratum-facing surface are shown. Bar, 10 μm. (B) The regions outlined by boxes in panel A are shown at higher magnification to highlight the clustering of ligand-bound integrins around zyxin-containing adhesions in GFP-positive cells. (C) Three-dimensional (3D) reconstructions from confocal *z* sections of representative cells from panel A are shown, revealing the distribution of zyxin (pseudostained red) and activated β1 integrins (pseudostained green). (D) Quantitative analysis of internalized β1 integrins. Integrin endocytosis assays were performed as described in the legend to panel A, but cell surface-bound 12G10 anti-β1 integrin antibodies were removed by acid stripping of cells before fixation. The immunofluorescence intensities of internalized β1 integrins were then measured and expressed in arbitrary units. The error bars indicate SEM ($n = 3$).

with this notion, two recent reports showed that the disassembly of focal adhesions in fibroblast cells (20) or of fibrillar adhesions in endothelial cells (52) occurs by endocytosis of α5β1 integrin from adhesion sites. Our findings extend the studies on focal adhesion disassembly by identifying PIPKIβ as a regulator of integrin endocytosis and by providing insight into how PIPKIβ regulates this process.

Our findings further identify dynamin 2 as a key effector of PIPKIβ. This notion is supported by loss of function mutations ($Dyn2^{PH}$) and by gain of function studies showing that dynamin 2 overexpression suppresses the phenotypic defects of PIPKIβ knockdown cells. Overexpression of dynamin 2 is likely to partially restore the targeting of this protein to adhesion sites because of the independent interaction mediated by its PRD domain with the FAK-Grb2 complex. As dynamin 2 regulates vesicle scission, a rate-liming step in endocytosis (48), this may provide one explanation of how dynamin 2 can overcome the loss of PIPKIβ. However, the finding that the $Dyn2^{PH}$ mutant is unable to do so suggests that $PI4,5P_2$ not only serves as a targeting signal, but also influences dynamin function by other means. Indeed, $PI4,5P_2$ is known to stimulate the GTPase activity of dynamin 2 (2, 36) and also promotes its oligomerization (31). The latter role is particularly intriguing, as dynamin oligomers are thought to induce the clustering of $PI4,5P_2$ in the membrane through its PH domain (3). Such a mechanism could explain how dynamin 2 is able to suppress the phenotypic defects of PIPKIβ-depleted cells and why the $Dyn2^{PH}$ mutant fails to do so, as dynamin 2 overexpression may lead to a local increase in $PI4,5P_2$ levels at focal adhesions, even in cells in which PIPKIβ levels are downregulated by RNAi. This, in turn, may partially restore clathrin assembly and endocytic vesicle scission to PIPKIβ-depleted cells, allowing focal adhesion disassembly.

The finding that overexpression of dynamin 2 restores directional cell migration to PIPKIβ-deficient cells further argues that PIPKIβ's role in cell motility is intimately linked to its modulation of endocytic trafficking. Emerging evidence suggests an intricate relationship between cell migration and endocytosis (11, 12, 42). Seminal work by Bretscher and colleagues has suggested that cell migration is the consequence of

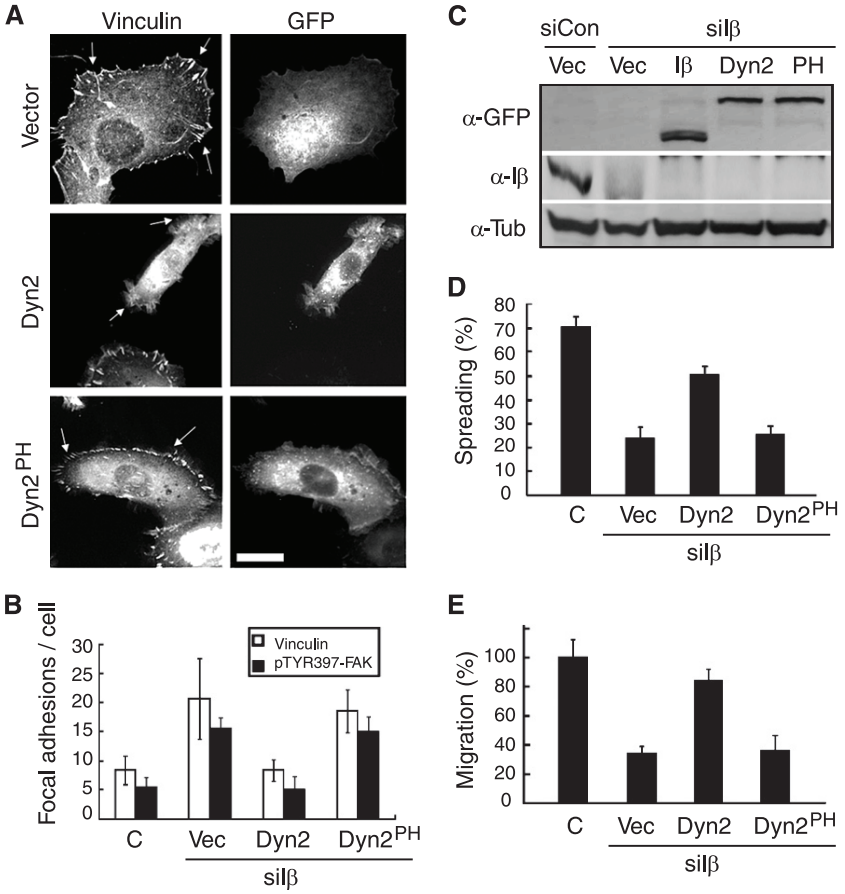

FIG. 15. Dynamin 2 suppresses the focal adhesion, cell-spreading, and migration defects of PIPKIβ knockdown cells. (A) Overexpression of dynamin 2, but not the Dyn2^{PH} mutant, suppresses the focal adhesion defect of PIPKIβ-depleted cells. PIPKIβ-depleted cells were transfected with plasmids encoding GFP (Vector), GFP-tagged wild-type dynamin 2 (Dyn2), or the dynamin Dyn2^{PH} mutant variant and immunostained with antibodies to vinculin (shown) or pY397-FAK (shown in panel B). GFP fluorescence was recorded directly. Representative examples of cells are shown. The arrows indicate enlarged peripheral focal adhesions. Bar, 10 μm. (B) Quantification of focal adhesion numbers from panel A. The values are means ± SEM from three independent experiments in which more than 250 cells were counted. (C) Western blot analysis of total cell lysates showing expression of transfected cDNAs and efficacy of PIPKIβ knockdown. As a control, tubulin levels remained constant. (D and E) Wild-type dynamin 2, but not the Dyn2^{PH} mutant, acts as a suppressor of the cell spreading and migration defects of PIPKIβ knockdown cells. PIPKIβ-depleted cells, transfected with the indicated plasmids, were assayed for cell spreading on fibronectin (D) and for cell migration toward 10% serum (E). The values are means plus SEM (n = 3).

a polarized endocytic and exocytic cycle that delivers membrane material and adhesion proteins for protrusion and substrate attachment to the leading edge of the migrating cell (5–8). The trafficking of integrins may thus play a key role in the development and maintenance of cell asymmetry. In line with this, PIPKIβ was recently implicated in the regulation of cell polarity development and chemotaxis in neutrophils (33). Our results corroborate the role of PIPKIβ in directed cell migration in a different model system and provide additional mechanistic insight into how PIPKIβ might regulate this process.

Finally, our findings provide strong evidence that functionally distinct pools of PI4,5P$_2$ are generated at adhesion sites through the specific actions of PIPKIβ and PIPKIγ661. Thus, an important yet-unsolved question from this work is how the function of PIPKIβ is controlled to allow the selective regulation of focal adhesion disassembly. Recent progress suggests that the unique C-terminal domain could represent a main functional feature distinguishing individual PIPKI isoforms from one another. This region in PIPKIγ661 not only mediates the specific interaction of PIPKIγ661 with talin, leading to the recruitment of PIPKIγ661 to focal adhesions, but also serves as a major site of posttranslational modification (18, 35, 37). Thus, it will be interesting to determine whether and how the C-terminal tail of PIPKIβ contributes to PIPKIβ's role in focal adhesion disassembly.

ACKNOWLEDGMENTS

We thank Mark McNiven, Sandra L. Schmid, Irina N. Kaverina, and Vic Small for the generous gifts of antibodies and plasmids and Jim Norman and Bernard Wehrle-Haller for reagents and discussion.

This work was supported by grants from the Dan Duncan Cancer Pilot Fund (J.K.) and the National Institutes of Health (GM068098 [J.K.], CA116097 [P.Z.], and HL077187 [M.E.D.]).

REFERENCES

1. **Achiriloaie, M., B. Barylko, and J. P. Albanesi.** 1999. Essential role of the dynamin pleckstrin homology domain in receptor-mediated endocytosis. Mol. Cell. Biol. **19:**1410–1415.

2. **Barylko, B., D. Binns, K. M. Lin, M. A. Atkinson, D. M. Jameson, H. L. Yin, and J. P. Albanesi.** 1998. Synergistic activation of dynamin GTPase by Grb2 and phosphoinositides. J. Biol. Chem. **273:**3791–3797.
3. **Bethoney, K. A., M. C. King, J. E. Hinshaw, E. M. Ostap, and M. A. Lemmon.** 2009. A possible effector role for the pleckstrin homology (PH) domain of dynamin. Proc. Natl. Acad. Sci. U. S. A. **106:**13359–13364.
4. **Bhatt, A., I. Kaverina, C. Otey, and A. Huttenlocher.** 2002. Regulation of focal complex composition and disassembly by the calcium-dependent protease calpain. J. Cell Sci. **115:**3415–3425.
5. **Bretscher, M. S.** 1989. Endocytosis and recycling of the fibronectin receptor in CHO cells. EMBO J. **8:**1341–1348.
6. **Bretscher, M. S.** 1996. Getting membrane flow and the cytoskeleton to cooperate in moving cells. Cell **87:**601–606.
7. **Bretscher, M. S.** 1996. Moving membrane up to the front of migrating cells. Cell **85:**465–467.
8. **Bretscher, M. S., and C. Aguado-Velasco.** 1998. Membrane traffic during cell locomotion. Curr. Opin. Cell Biol. **10:**537–541.
9. **Broussard, J. A., D. J. Webb, and I. Kaverina.** 2008. Asymmetric focal adhesion disassembly in motile cells. Curr. Opin. Cell Biol. **20:**85–90.
10. **Burridge, K., S. K. Sastry, and J. L. Sallee.** 2006. Regulation of cell adhesion by protein-tyrosine phosphatases. I. Cell-matrix adhesion. J. Biol. Chem. **281:**15593–15596.
11. **Caswell, P. T., M. Chan, A. J. Lindsay, M. W. McCaffrey, D. Boettiger, and J. C. Norman.** 2008. Rab-coupling protein coordinates recycling of alpha5beta1 integrin and EGFR1 to promote cell migration in 3D microenvironments. J. Cell Biol. **183:**143–155.
12. **Caswell, P. T., H. J. Spence, M. Parsons, D. P. White, K. Clark, K. W. Cheng, G. B. Mills, M. J. Humphries, A. J. Messent, K. I. Anderson, M. W. McCaffrey, B. W. Ozanne, and J. C. Norman.** 2007. Rab25 associates with alpha5beta1 integrin to promote invasive migration in 3D microenvironments. Dev. Cell **13:**496–510.
13. **Chandrasekar, I., T. E. Stradal, M. R. Holt, F. Entschladen, B. M. Jockusch, and W. H. Ziegler.** 2005. Vinculin acts as a sensor in lipid regulation of adhesion-site turnover. J. Cell Sci. **118:**1461–1472.
14. **Chao, W. T., and J. Kunz.** 2009. Focal adhesion disassembly requires clathrin-dependent endocytosis of integrins. FEBS Lett. **583:**1337–1343.
15. **Chavrier, P., R. G. Parton, H. P. Hauri, K. Simons, and M. Zerial.** 1990. Localization of low molecular weight GTP binding proteins to exocytic and endocytic compartments. Cell **62:**317–329.
16. **Coppolino, M. G., R. Dierckman, J. Loijens, R. F. Collins, M. Pouladi, J. Jongstra-Bilen, A. D. Schreiber, W. S. Trimble, R. Anderson, and S. Grinstein.** 2002. Inhibition of phosphatidylinositol-4-phosphate 5-kinase Ialpha impairs localized actin remodeling and suppresses phagocytosis. J. Biol. Chem. **277:**43849–43857.
17. **Di Paolo, G., and P. De Camilli.** 2006. Phosphoinositides in cell regulation and membrane dynamics. Nature **443:**651–657.
18. **Di Paolo, G., L. Pellegrini, K. Letinic, G. Cestra, R. Zoncu, S. Voronov, S. Chang, J. Guo, M. R. Wenk, and P. De Camilli.** 2002. Recruitment and regulation of phosphatidylinositol phosphate kinase type 1 gamma by the FERM domain of talin. Nature **420:**85–89.
19. **Doughman, R. L., A. D. Firestone, M. W. Wojtasiak, and R. A. Anderson.** 2003. Membrane ruffling requires coordination between type Iα phosphatidylinositol phosphate kinase and Rac signaling. J. Biol. Chem. **278:**23036–23045.
20. **Ezratty, E. J., C. Bertaux, E. E. Marcantonio, and G. G. Gundersen.** 2009. Clathrin mediates integrin endocytosis for focal adhesion disassembly in migrating cells. J. Cell Biol. **187:**733–747.
21. **Ezratty, E. J., M. A. Partridge, and G. G. Gundersen.** 2005. Microtubule-induced focal adhesion disassembly is mediated by dynamin and focal adhesion kinase. Nat. Cell Biol. **7:**581–590.
22. **Franco, S. J., M. A. Rodgers, B. J. Perrin, J. Han, D. A. Bennin, D. R. Critchley, and A. Huttenlocher.** 2004. Calpain-mediated proteolysis of talin regulates adhesion dynamics. Nat. Cell Biol. **6:**977–983.
23. **Gilmore, A. P., and K. Burridge.** 1996. Regulation of vinculin binding to talin and actin by phosphatidyl-inositol-4-5-bisphosphate. Nature **381:**531–535.
24. **Hauck, C. R., D. A. Hsia, and D. D. Schlaepfer.** 2002. The focal adhesion kinase—a regulator of cell migration and invasion. IUBMB Life **53:**115–119.
25. **Haucke, V.** 2005. Phosphoinositide regulation of clathrin-mediated endocytosis. Biochem. Soc. Trans. **33:**1285–1289.
26. **Ilić, D., Y. Furuta, S. Kanazawa, N. Takeda, K. Sobue, N. Nakatsuji, S. Nomura, J. Fujimoto, M. Okada, and T. Yamamoto.** 1995. Reduced cell motility and enhanced focal adhesion contact formation in cells from FAK-deficient mice. Nature **377:**539–544.
27. **Ishihara, H., Y. Shibasaki, N. Kizuki, H. Katagiri, Y. Yazaki, T. Asano, and Y. Oka.** 1996. Cloning of cDNAs encoding two isoforms of 68-kDa type I phosphatidylinositol-4-phosphate 5-kinase. J. Biol. Chem. **271:**23611–23614.
28. **Ishihara, H., Y. Shibasaki, N. Kizuki, T. Wada, Y. Yazaki, T. Asano, and Y. Oka.** 1998. Type I phosphatidylinositol-4-phosphate 5-kinases. Cloning of the third isoform and deletion/substitution analysis of members of this novel lipid kinase family. J. Biol. Chem. **273:**8741–8748.
29. **Jović, M., N. Naslavsky, D. Rapaport, M. Horowitz, and S. Caplan.** 2007. EHD1 regulates beta1 integrin endosomal transport: effects on focal adhesions, cell spreading and migration. J. Cell Sci. **120:**802–814.
30. **Kaverina, I., O. Krylyshkina, and J. V. Small.** 2002. Regulation of substrate adhesion dynamics during cell motility. Int. J. Biochem. Cell Biol. **34:**746–761.
31. **Klein, D. E., A. Lee, D. W. Frank, M. S. Marks, and M. A. Lemmon.** 1998. The pleckstrin homology domains of dynamin isoforms require oligomerization for high affinity phosphoinositide binding. J. Biol. Chem. **273:**27725–27733.
32. **Kunz, J., M. P. Wilson, M. Kisseleva, J. H. Hurley, P. W. Majerus, and R. A. Anderson.** 2000. The activation loop of phosphatidylinositol phosphate kinases determines signaling specificity. Mol. Cell **5:**1–11.
33. **Lacalle, R. A., R. M. Peregil, J. P. Albar, E. Merino, A. C. Martinez, I. Merida, and S. Manes.** 2007. Type I phosphatidylinositol 4-phosphate 5-kinase controls neutrophil polarity and directional movement. J. Cell Biol. **179:**1539–1553.
34. **Laukaitis, C. M., D. J. Webb, K. Donais, and A. F. Horwitz.** 2001. Differential dynamics of alpha 5 integrin, paxillin, and alpha-actinin during formation and disassembly of adhesions in migrating cells. J. Cell Biol. **153:**1427–1440.
35. **Lee, S. Y., S. Voronov, K. Letinic, A. C. Nairn, G. Di Paolo, and P. De Camilli.** 2005. Regulation of the interaction between PIPKI gamma and talin by proline-directed protein kinases. J. Cell Biol. **168:**789–799.
36. **Lin, H. C., B. Barylko, M. Achiriloaie, and J. P. Albanesi.** 1997. Phosphatidylinositol (4,5)-bisphosphate-dependent activation of dynamins I and II lacking the proline/arginine-rich domains. J. Biol. Chem. **272:**25999–26004.
37. **Ling, K., R. L. Doughman, A. J. Firestone, M. W. Bunce, and R. A. Anderson.** 2002. Type I gamma phosphatidylinositol phosphate kinase targets and regulates focal adhesions. Nature **420:**89–93.
38. **Ling, K., N. J. Schill, M. P. Wagoner, Y. Sun, and R. A. Anderson.** 2006. Movin' on up: the role of PtdIns(4,5)P(2) in cell migration. Trends Cell Biol. **16:**276–284.
39. **Loijens, J. C., and R. A. Anderson.** 1996. Type I phosphatidylinositol-4-phosphate 5-kinases are distinct members of this novel lipid kinase family. J. Biol. Chem. **271:**32937–32943.
40. **McNamee, H. P., H. G. Liley, and D. E. Ingber.** 1996. Integrin-dependent control of inositol lipid synthesis in vascular endothelial cells and smooth muscle cells. Exp. Cell Res. **224:**116–122.
41. **Nishimura, T., and K. Kaibuchi.** 2007. Numb controls integrin endocytosis for directional cell migration with aPKC and PAR-3. Dev. Cell **13:**15–28.
42. **Prigozhina, N. L., and C. M. Waterman-Storer.** 2006. Decreased polarity and increased random motility in PtK1 epithelial cells correlate with inhibition of endosomal recycling. J. Cell Sci. **119:**3571–3582.
43. **Ramachandran, R., and S. L. Schmid.** 2008. Real-time detection reveals that effectors couple dynamin's GTP-dependent conformational changes to the membrane. EMBO J. **27:**27–37.
44. **Ren, X. D., and M. A. Schwartz.** 2000. Determination of GTP loading on Rho. Methods Enzymol. **325:**264–272.
45. **Roberts, M., S. Barry, A. Woods, P. van der Sluijs, and J. Norman.** 2001. PDGF-regulated rab4-dependent recycling of alphavbeta3 integrin from early endosomes is necessary for cell adhesion and spreading. Curr. Biol. **11:**1392–1402.
46. **Saunders, R. M., M. R. Holt, L. Jennings, D. H. Sutton, I. L. Barsukov, A. Bobkov, R. C. Liddington, E. A. Adamson, G. A. Dunn, and D. R. Critchley.** 2006. Role of vinculin in regulating focal adhesion turnover. Eur. J. Cell Biol. **85:**487–500.
47. **Sechi, A. S., and J. Wehland.** 2000. The actin cytoskeleton and plasma membrane connection: PtdIns(4,5)P(2) influences cytoskeletal protein activity at the plasma membrane. J. Cell Sci. **113:**3685–3695.
48. **Sever, S., H. Damke, and S. L. Schmid.** 2000. Dynamin:GTP controls the formation of constricted coated pits, the rate limiting step in clathrin-mediated endocytosis. J. Cell Biol. **150:**1137–1148.
49. **Shibasaki, Y., H. Ishihara, N. Kizuki, T. Asano, Y. Oka, and Y. Yazaki.** 1997. Massive actin polymerization induced by phosphatidylinositol-4-phosphate 5-kinase in vivo. J. Biol. Chem. **272:**7578–7581.
50. **Sottile, J., D. C. Hocking, and P. J. Swiatek.** 1998. Fibronectin matrix assembly enhances adhesion-dependent cell growth. J. Cell Sci. **111:**2933–2943.
51. **Takenawa, T., and T. Itoh.** 2001. Phosphoinositides, key molecules for regulation of actin cytoskeletal organization and membrane traffic from the plasma membrane. Biochim. Biophys. Acta **1533:**190–206.
52. **Valdembri, D., P. T. Caswell, K. I. Anderson, J. P. Schwarz, I. Konig, E. Astanina, F. Caccavari, J. C. Norman, M. J. Humphries, F. Bussolino, and G. Serini.** 2009. Neuropilin-1/GIPC1 signaling regulates alpha5beta1 integrin traffic and function in endothelial cells. PLoS Biol. **7:**e25.
53. **Vallis, Y., P. Wigge, B. Marks, P. R. Evans, and H. T. McMahon.** 1999. Importance of the pleckstrin homology domain of dynamin in clathrin-mediated endocytosis. Curr. Biol. **9:**257–260.
54. **Volberg, T., B. Geiger, Z. Kam, R. Pankov, I. Simcha, H. Sabanay, J. L. Coll,**

E. Adamson, and A. Ben-Ze'ev. 1995. Focal adhesion formation by F9 embryonal carcinoma cells after vinculin gene disruption. J. Cell Sci. **108:**2253–2260.

55. **Webb, D. J., K. Donais, L. A. Whitmore, S. M. Thomas, C. E. Turner, J. T. Parsons, and A. F. Horwitz.** 2004. FAK-Src signalling through paxillin, ERK and MLCK regulates adhesion disassembly. Nat. Cell Biol. **6:**154–161.
56. **Webb, D. J., J. T. Parsons, and A. F. Horwitz.** 2002. Adhesion assembly, disassembly and turnover in migrating cells—over and over and over again. Nat. Cell Biol. **4:**E97–E100.
57. **Yin, H. L., and P. A. Janmey.** 2003. Phosphoinositide regulation of the actin cytoskeleton. Annu. Rev. Physiol. **65:**761–789.
58. **Zoncu, R., R. M. Perera, R. Sebastian, F. Nakatsu, H. Chen, T. Balla, G. Ayala, D. Toomre, and P. V. De Camilli.** 2007. Loss of endocytic clathrin-coated pits upon acute depletion of phosphatidylinositol 4,5-bisphosphate. Proc. Natl. Acad. Sci. U. S. A. **104:**3793–3798.